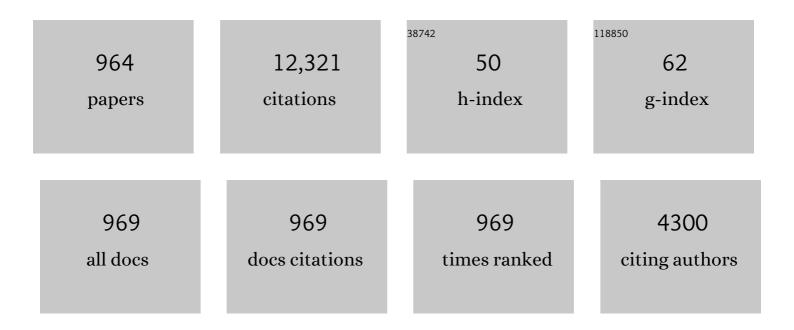
List of Publications by Year in descending order

Source: https://exaly.com/author-pdf/9517225/publications.pdf Version: 2024-02-01



#	Article	IF	CITATIONS
1	Current sensor based on microfiber knot resonator. Sensors and Actuators A: Physical, 2011, 167, 60-62.	4.1	120
2	Generation of Mode-Locked Ytterbium Doped Fiber Ring Laser Using Few-Layer Black Phosphorus as a Saturable Absorber. IEEE Journal of Selected Topics in Quantum Electronics, 2017, 23, 39-43.	2.9	105
3	C-Band Q-Switched Fiber Laser Using Titanium Dioxide (TiO 2) As Saturable Absorber. IEEE Photonics Journal, 2016, 8, 1-7.	2.0	92
4	Gain enhancement in L-band EDFA through a double-pass technique. IEEE Photonics Technology Letters, 2002, 14, 296-297.	2.5	86
5	Zinc oxide (ZnO) nanoparticles as saturable absorber in passively Q-switched fiber laser. Optics Communications, 2016, 381, 72-76.	2.1	85
6	Theoretical analysis and fabrication of tapered fiber. Optik, 2013, 124, 538-543.	2.9	83
7	Black phosphorus crystal as a saturable absorber for both a Q-switched and mode-locked erbium-doped fiber laser. RSC Advances, 2016, 6, 72692-72697.	3.6	83
8	Tapered plastic multimode fiber sensor for salinity detection. Sensors and Actuators A: Physical, 2011, 171, 219-222.	4.1	79
9	A review of recent developed and applications of plastic fiber optic displacement sensors. Measurement: Journal of the International Measurement Confederation, 2014, 48, 333-345.	5.0	74
10	A Stable Dual-wavelength Thulium-doped Fiber Laser at 1.9 μm Using Photonic Crystal Fiber. Scientific Reports, 2015, 5, 14537.	3.3	73
11	Titanium Dioxide (TiO 2) film as a new saturable absorber for generating mode-locked Thulium-Holmium doped all-fiber laser. Optics and Laser Technology, 2017, 89, 16-20.	4.6	72
12	Multiwavelength Brillouin/Erbium-Ytterbium fiber laser. Laser Physics Letters, 2007, 4, 601-603.	1.4	71
13	An overview on S-band erbium-doped fiber amplifiers. Laser Physics Letters, 2007, 4, 10-15.	1.4	70
14	A linear cavity Brillouin fiber laser with multiple wavelengths output. Laser Physics Letters, 2008, 5, 361-363.	1.4	70
15	FBG Sensors for Environmental and Biochemical Applications—A Review. IEEE Sensors Journal, 2020, 20, 7614-7627.	4.7	70
16	Gain clamping in L-band erbium-doped fiber amplifier using a fiber Bragg grating. IEEE Photonics Technology Letters, 2002, 14, 293-295.	2.5	69
17	A Q-Switched Erbium-Doped Fiber Laser with a Carbon Nanotube Based Saturable Absorber. Chinese Physics Letters, 2012, 29, 114202.	3.3	67
18	Passively Q-switched Erbium-doped and Ytterbium-doped fibre lasers with topological insulator bismuth selenide (Bi2Se3) as saturable absorber. Optics and Laser Technology, 2017, 88, 121-127.	4.6	66

#	Article	IF	CITATIONS
19	Double-pass L-band EDFA with enhanced noise figure characteristics. IEEE Photonics Technology Letters, 2003, 15, 1055-1057.	2.5	64
20	Tunable dual wavelength fiber laser incorporating AWG and optical channel selector by controlling the cavity loss. Optics Communications, 2009, 282, 4771-4775.	2.1	63
21	Multiple wavelength Brillouin fiber laser from injection of intense signal light. Laser Physics Letters, 2007, 4, 678-680.	1.4	62
22	Multi-wavelength Brillouin fiber laser using Brillouin-Rayleigh scatterings in distributed Raman amplifier. Laser Physics Letters, 2009, 6, 737-739.	1.4	62
23	SOA-based quad-wavelength ring laser. Laser Physics Letters, 2008, 5, 726-729.	1.4	61
24	0.16nm spaced multi-wavelength Brillouin fiber laser in a figure-of-eight configuration. Optics and Laser Technology, 2011, 43, 866-869.	4.6	61
25	Integrated Microfibre Device for Refractive Index and Temperature Sensing. Sensors, 2012, 12, 11782-11789.	3.8	61
26	An efficient S-band erbium-doped fiber amplifier using double-pass configuration. IEICE Electronics Express, 2005, 2, 182-185.	0.8	60
27	Bismuth-based erbium-doped fiber as a gain medium for L-band amplification and Brillouin fiber laser. Laser Physics, 2010, 20, 716-719.	1.2	60
28	Multi-wavelength fiber laser in the S-band region using a Sagnac loop mirror as a comb generator in an SOA gain medium. Laser Physics Letters, 2010, 7, 673-676.	1.4	60
29	Passively Q-switched erbium-doped fiber laser at C-band region based on WS_2 saturable absorber. Applied Optics, 2016, 55, 1001.	2.1	60
30	A linear cavity S-band Brillouin/Erbium fiber laser. Laser Physics Letters, 2006, 3, 369-371.	1.4	59
31	Multi-wavelength erbium-doped fiber laser assisted by four-wave mixing effect. Laser Physics Letters, 2009, 6, 813-815.	1.4	59
32	Compact Brillouin–erbium fiber laser. Optics Letters, 2009, 34, 46.	3.3	59
33	2.0-\$muhbox{m}\$ Q-Switched Thulium-Doped Fiber Laser With Graphene Oxide Saturable Absorber. IEEE Photonics Journal, 2013, 5, 1501108-1501108.	2.0	59
34	High power and compact switchable bismuth based multiwavelength fiber laser. Laser Physics Letters, 2009, 6, 380-383.	1.4	58
35	Latex micro-balloon pumping in centrifugal microfluidic platforms. Lab on A Chip, 2014, 14, 988.	6.0	58
36	A Study of Relative Humidity Fiber-Optic Sensors. IEEE Sensors Journal, 2015, 15, 1945-1950.	4.7	58

#	Article	IF	CITATIONS
37	An efficient gain-flattened C-band Erbium-doped fiber amplifier. Laser Physics Letters, 2006, 3, 536-538.	1.4	57
38	A new configuration of multi-wavelength Brillouin fiber laser. Laser Physics Letters, 2008, 5, 48-50.	1.4	56
39	Nanosecond soliton pulse generation by mode-locked erbium-doped fiber laser using single-walled carbon-nanotube-based saturable absorber. Applied Optics, 2012, 51, 8621.	1.8	56
40	Linear cavity Brillouin fiber laser with improved characteristics. Optics Letters, 2008, 33, 770.	3.3	55
41	Flatly broadened supercontinuum generation in nonlinear fibers using a mode locked bismuth oxide based erbium doped fiber laser. Laser Physics Letters, 2011, 8, 369-375.	1.4	55
42	Tapered plastic optical fiber coated with ZnO nanostructures for the measurement of uric acid concentrations and changes in relative humidity. Sensors and Actuators A: Physical, 2014, 210, 190-196.	4.1	54
43	Optical Fiber Relative Humidity Sensor Based on Inline Mach–Zehnder Interferometer With ZnO Nanowires Coating. IEEE Sensors Journal, 2016, 16, 312-316.	4.7	54
44	Fibre Optic Sensors for Selected Wastewater Characteristics. Sensors, 2013, 13, 8640-8668.	3.8	53
45	Nickel oxide nanoparticles as a saturable absorber for an all-fiber passively Q-switched erbium-doped fiber laser. Laser Physics, 2017, 27, 065105.	1.2	53
46	Investigation of cladding thicknesses on silver SPR based side-polished optical fiber refractive-index sensor. Results in Physics, 2019, 13, 102255.	4.1	53
47	MAX phase based saturable absorber for mode-locked erbium-doped fiber laser. Optics and Laser Technology, 2020, 127, 106186.	4.6	53
48	Multi-wavelength Brillouin fiber laser using a holey fiber and a bismuth-oxide based erbium-doped fiber. Laser Physics Letters, 2009, 6, 454-457.	1.4	52
49	S-band erbium-doped fiber ring laser using a fiber Bragg grating. Laser Physics Letters, 2005, 2, 369-371.	1.4	51
50	S-band Brillouin erbium fibre laser. Electronics Letters, 2005, 41, 174.	1.0	51
51	A <i>Q</i> -switched erbium-doped fiber laser with a graphene saturable absorber. Laser Physics Letters, 2013, 10, 025102.	1.4	51
52	S-band Q-switched fiber laser using MoSe 2 saturable absorber. Optics Communications, 2017, 382, 93-98.	2.1	51
53	The performance of a fiber optic displacement sensor for different types of probes and targets. Laser Physics Letters, 2008, 5, 55-58.	1.4	50
54	Tunable Q-switched fiber laser using zinc oxide nanoparticles as a saturable absorber. Applied Optics, 2016, 55, 4277.	2.1	50

#	Article	IF	CITATIONS
55	Ultrafast erbium-doped fiber laser mode-locked with a black phosphorus saturable absorber. Laser Physics Letters, 2016, 13, 095104.	1.4	49
56	FIrpic thin film as saturable absorber for passively Q-switched and mode-locked erbium-doped fiber laser. Optical Fiber Technology, 2019, 50, 256-262.	2.7	49
57	Mode-locked bismuth-based erbium-doped fiber laser with stable and clean femtosecond pulses output. Laser Physics Letters, 2011, 8, 449-452.	1.4	48
58	Relative Humidity Sensing Using a PMMA Doped Agarose Gel Microfiber. Journal of Lightwave Technology, 2017, 35, 3940-3944.	4.6	48
59	A PMMA microfiber loop resonator based humidity sensor with ZnO nanorods coating. Measurement: Journal of the International Measurement Confederation, 2017, 99, 128-133.	5.0	47
60	All-fiber dual-wavelength Q-switched and mode-locked EDFL by SMF-THDF-SMF structure as a saturable absorber. Optics Communications, 2017, 389, 29-34.	2.1	47
61	Conducting polymer coated optical microfiber sensor for alcohol detection. Sensors and Actuators A: Physical, 2014, 205, 58-62.	4.1	45
62	Refractive index sensor based on SPR in symmetrically etched plastic optical fibers. Sensors and Actuators A: Physical, 2016, 246, 163-169.	4.1	45
63	Copper oxide nanomaterial saturable absorber as a new passive Q-switcher in erbium-doped fiber laser ring cavity configuration. Results in Physics, 2018, 10, 264-269.	4.1	45
64	Microfiber loop resonator based temperature sensor. Journal of the European Optical Society-Rapid Publications, 0, 6, .	1.9	44
65	Ultrashort pulse generation with an erbium-doped fiber laser ring cavity based on a copper oxide saturable absorber. Applied Optics, 2018, 57, 5180.	1.8	44
66	Wideband EDFA Based on Erbium Doped Crystalline Zirconia Yttria Alumino Silicate Fiber. Journal of Lightwave Technology, 2010, 28, 2919-2924.	4.6	43
67	Application of multiple linear regression, central composite design, and ANFIS models in dye concentration measurement and prediction using plastic optical fiber sensor. Measurement: Journal of the International Measurement Confederation, 2015, 74, 78-86.	5.0	43
68	Q-switched erbium doped fiber laser based on single and multiple walled carbon nanotubes embedded in polyethylene oxide film as saturable absorber. Optics and Laser Technology, 2015, 65, 25-28.	4.6	42
69	Q-switched Erbium-doped fiber laser using MoSe 2 as saturable absorber. Optics and Laser Technology, 2016, 79, 20-23.	4.6	42
70	Fiber-Optic Salinity Sensor Using Fiber-Optic Displacement Measurement With Flat and Concave Mirror. IEEE Journal of Selected Topics in Quantum Electronics, 2012, 18, 1529-1533.	2.9	41
71	Inline Microfiber Mach–Zehnder Interferometer for High Temperature Sensing. IEEE Sensors Journal, 2013, 13, 626-628.	4.7	41
72	Refractive index and strain sensing using inline Mach–Zehnder interferometer comprising perfluorinated graded-index plastic optical fiber. Sensors and Actuators A: Physical, 2014, 219, 94-99.	4.1	41

#	Article	IF	CITATIONS
73	Q-Switched Ytterbium-Doped Fiber Laser Using Black Phosphorus as Saturable Absorber. Chinese Physics Letters, 2016, 33, 054206.	3.3	41
74	Wide-Band Bismuth-Based Erbium-Doped Fiber Amplifier With a Flat-Gain Characteristic. IEEE Photonics Journal, 2009, 1, 259-264.	2.0	40
75	Resonance condition of a microfiber knot resonator immersed in liquids. Applied Optics, 2011, 50, 5912.	2.1	40
76	Polyaniline (PAni) optical sensor in chloroform detection. Sensors and Actuators B: Chemical, 2018, 261, 97-105.	7.8	40
77	High Sensitivity Fiber Bragg Grating Pressure Sensor Using Thin Metal Diaphragm. IEEE Sensors Journal, 2009, 9, 1654-1659.	4.7	39
78	S-band multiwavelength ring Brillouin/Raman fiber laser with 20 GHz channel spacing. Applied Optics, 2012, 51, 1811.	1.8	39
79	Fiber Optic Displacement Sensor for Temperature Measurement. IEEE Sensors Journal, 2012, 12, 1361-1364.	4.7	39
80	Non-adiabatic silica microfiber for strain and temperature sensors. Sensors and Actuators A: Physical, 2013, 192, 130-132.	4.1	39
81	Experimental realization and performance evaluation of refractive index SPR sensor based on unmasked short tapered multimode-fiber operating in aqueous environments. Sensors and Actuators A: Physical, 2015, 236, 38-43.	4.1	39
82	Highâ€sensitivity pressure sensor using a polymerâ€embedded FBG. Microwave and Optical Technology Letters, 2008, 50, 60-61.	1.4	38
83	Performance comparison of Zr-based and Bi-based erbium-doped fiber amplifiers. Optics Letters, 2010, 35, 2882.	3.3	38
84	Biosensing enhancement of dengue virus using microballoon mixers on centrifugal microfluidic platforms. Biosensors and Bioelectronics, 2015, 67, 424-430.	10.1	38
85	Tapered Plastic Optical Fiber Coated With Al-Doped ZnO Nanostructures for Detecting Relative Humidity. IEEE Sensors Journal, 2015, 15, 845-849.	4.7	38
86	Highly responsive NaCl detector based on inline microfiber Mach–Zehnder interferometer. Sensors and Actuators A: Physical, 2016, 237, 56-61.	4.1	38
87	Mode-Locked Erbium-Doped Fiber Laser Using Vanadium Oxide as Saturable Absorber. Chinese Physics Letters, 2018, 35, 044204.	3.3	38
88	Bidirectional multiwavelength Brillouin fiber laser generation in a ring cavity. Journal of Optics, 2008, 10, 055101.	1.5	37
89	Passively Q-switched and mode-locked Erbium-doped fiber laser with topological insulator Bismuth Selenide (Bi2Se3) as saturable absorber at C-band region. Optical Fiber Technology, 2019, 48, 117-122.	2.7	37
90	Graphene-Based Saturable Absorber for Single-Longitudinal-Mode Operation of Highly Doped Erbium-Doped Fiber Laser. IEEE Photonics Journal, 2012, 4, 467-475.	2.0	36

#	Article	IF	CITATIONS
91	Tapered Plastic Optical Fiber Coated With Graphene for Uric Acid Detection. IEEE Sensors Journal, 2014, 14, 1704-1709.	4.7	36
92	A black phosphorus-based tunable Q-switched ytterbium fiber laser. Laser Physics Letters, 2016, 13, 095103.	1.4	36
93	Femtosecond mode-locked erbium-doped fiber laser based on MoS2–PVA saturable absorber. Optics and Laser Technology, 2016, 82, 145-149.	4.6	36
94	All-optical gain-clamped erbium-doped fiber-ring lasing amplifier with laser filtering technique. IEEE Photonics Technology Letters, 2001, 13, 785-787.	2.5	35
95	An efficient multiwavelength light source based on ASE slicing. Laser Physics Letters, 2006, 3, 495-497.	1.4	35
96	Q-switched and mode-locked thulium doped fiber lasers with nickel oxide film saturable absorber. Optics Communications, 2019, 447, 6-12.	2.1	35
97	Graphene-Oxide-Based Saturable Absorber for All-Fiber Q-Switching With a Simple Optical Deposition Technique. IEEE Photonics Journal, 2012, 4, 2205-2213.	2.0	34
98	Optical Fiber Sensing of Salinity and Liquid Level. IEEE Photonics Technology Letters, 2014, 26, 1742-1745.	2.5	34
99	Q-switched and mode-locked thulium-doped fiber laser with pure Antimony film Saturable absorber. Optics Communications, 2018, 421, 99-104.	2.1	34
100	Spacing-Switchable Multiwavelength Fiber Laser Based on Nonlinear Polarization Rotation and Brillouin Scattering in Photonic Crystal Fiber. IEEE Photonics Journal, 2012, 4, 34-38.	2.0	33
101	Distributed feedback multimode Brillouin–Raman random fiber laser in the S-band. Laser Physics Letters, 2013, 10, 055102.	1.4	33
102	S-band Q-switched fiber laser using molybdenum disulfide (MoS ₂) saturable absorber. Laser Physics Letters, 2016, 13, 035103.	1.4	33
103	Zinc Oxide-Based Q-Switched Erbium-Doped Fiber Laser. Chinese Physics Letters, 2017, 34, 044202.	3.3	33
104	Multi-wavelength bismuth-based erbium-doped fiber laser based on four-wave mixing effect in photonic crystal fiber. Optics and Laser Technology, 2010, 42, 1250-1252.	4.6	32
105	Reversible thermo-pneumatic valves on centrifugal microfluidic platforms. Lab on A Chip, 2015, 15, 3358-3369.	6.0	32
106	SOA-based multi-wavelength laser using fiber Bragg gratings. Laser Physics, 2009, 19, 1002-1005.	1.2	31
107	WIDE-BAND HYBRID AMPLIFIER OPERATING IN S-BAND REGION. Progress in Electromagnetics Research, 2010, 102, 301-313.	4.4	31
108	Controlled side coupling of light to cladding mode of ZnO nanorod coated optical fibers and its implications for chemical vapor sensing. Sensors and Actuators B: Chemical, 2014, 202, 543-550.	7.8	31

#	Article	IF	CITATIONS
109	Q-Switching Pulse Operation in 1.5-î¼m Region Using Copper Nanoparticles as Saturable Absorber. Chinese Physics Letters, 2017, 34, 034205.	3.3	31
110	FWM-based multi-wavelength erbium-doped fiber laser using Bi-EDF. Laser Physics, 2010, 20, 1414-1417.	1.2	30
111	Micro-Ball Lensed Fiber-Based Glucose Sensor. IEEE Sensors Journal, 2013, 13, 348-350.	4.7	30
112	Optical frequency comb generation based on chirping of Mach–Zehnder Modulators. Optics Communications, 2015, 344, 139-146.	2.1	30
113	Electrically Tunable Microfiber Knot Resonator Based Erbium-Doped Fiber Laser. IEEE Journal of Quantum Electronics, 2012, 48, 443-446.	1.9	29
114	Narrow Spacing Dual-Wavelength Fiber Laser Based on Polarization Dependent Loss Control. IEEE Photonics Journal, 2013, 5, 1502706-1502706.	2.0	29
115	Graphene-Based Mode-Locked Spectrum-Tunable Fiber Laser Using Mach–Zehnder Filter. IEEE Photonics Journal, 2013, 5, 1501709-1501709.	2.0	29
116	Photonic crystal fiber based dual-wavelength Q-switched fiber laser using graphene oxide as a saturable absorber. Applied Optics, 2014, 53, 3581.	1.8	29
117	All fiber mode-locked Erbium-doped fiber laser using single-walled carbon nanotubes embedded into polyvinyl alcohol film as saturable absorber. Optics and Laser Technology, 2014, 62, 40-43.	4.6	29
118	A Switchable Figure Eight Erbium-Doped Fiber Laser Based on Inter-Modal Beating By Means of Non-Adiabatic Microfiber. Journal of Lightwave Technology, 2015, 33, 528-534.	4.6	29
119	Silver nanoparticle-film based saturable absorber for passively <i>Q</i> -switched erbium-doped fiber laser (EDFL) in ring cavity configuration. Laser Physics, 2016, 26, 095103.	1.2	29
120	Generation of soliton and bound soliton pulses in mode-locked erbium-doped fiber laser using graphene film as saturable absorber. Journal of Modern Optics, 2016, 63, 777-782.	1.3	29
121	Tunable graphene-based Q-switched erbium-doped fiber laser using fiber Bragg grating. Journal of Modern Optics, 2013, 60, 202-212.	1.3	28
122	Tunable S-Band Q-Switched Fiber Laser Using Bi ₂ Se ₃ as the Saturable Absorber. IEEE Photonics Journal, 2015, 7, 1-8.	2.0	28
123	Titanium dioxide doped fiber as a new saturable absorber for generating mode-locked erbium doped fiber laser. Optik, 2018, 158, 1327-1333.	2.9	28
124	Applied microfiber evanescent wave on ZnO nanorods coated glass surface towards temperature sensing. Sensors and Actuators A: Physical, 2018, 277, 103-111.	4.1	28
125	Comparison of performances between partial double-pass and full double-pass systems in two-stage L-band EDFA. Laser Physics Letters, 2004, 1, 610-612.	1.4	27
126	Domain-wall dark pulse generation in fiber laser incorporating MoS2. Applied Physics B: Lasers and Optics, 2016, 122, 1.	2.2	27

#	Article	IF	CITATIONS
127	PMMA microfiber loop resonator for humidity sensor. Sensors and Actuators A: Physical, 2017, 260, 112-116.	4.1	27
128	Multi-walled carbon nanotubes doped Poly(Methyl MethAcrylate) microfiber for relative humidity sensing. Sensors and Actuators A: Physical, 2018, 272, 274-280.	4.1	27
129	A few-picosecond and high-peak-power passively mode-locked erbium-doped fibre laser based on zinc oxide polyvinyl alcohol film saturable absorber. Laser Physics, 2018, 28, 075105.	1.2	27
130	Holmium oxide thin film as a saturable absorber for generating Q-switched and mode-locked erbium-doped fiber lasers. Optical Fiber Technology, 2019, 52, 101996.	2.7	27
131	Generation of Q-switched and mode-locked pulses with Eu2O3 saturable absorber. Optics and Laser Technology, 2020, 127, 106163.	4.6	27
132	Current sensor based on inline microfiber Mach–Zehnder interferometer. Sensors and Actuators A: Physical, 2013, 192, 9-12.	4.1	26
133	Study of a fiber optic humidity sensor based on agarose gel. Journal of Modern Optics, 2014, 61, 244-248.	1.3	26
134	A generation of 2Âμm Q-switched thulium-doped fibre laser based on anatase titanium(IV) oxide film saturable absorber. Journal of Modern Optics, 2017, 64, 187-190.	1.3	26
135	Ultrashort Pulse Soliton Fiber Laser Generation With Integration of Antimony Film Saturable Absorber. Journal of Lightwave Technology, 2018, 36, 3522-3527.	4.6	26
136	Investigation of Surface Plasmon Resonance (SPR) in MoS2- and WS2-Protected Titanium Side-Polished Optical Fiber as a Humidity Sensor. Micromachines, 2019, 10, 465.	2.9	26
137	Tungsten trioxide (WO3) film absorber for generating soliton mode-locked pulses in erbium laser. Optics and Laser Technology, 2020, 131, 106429.	4.6	26
138	Multi-wavelength generation using a bismuth-based EDF and Brillouin effect in a linear cavity configuration. Optics and Laser Technology, 2009, 41, 198-201.	4.6	25
139	Temperature-sensitive dual-segment polarization maintaining fiber Sagnac loop mirror. Optics and Laser Technology, 2010, 42, 377-381.	4.6	25
140	Theoretical and experimental study on the fiber optic displacement sensor with two receiving fibers. Microwave and Optical Technology Letters, 2010, 52, 373-375.	1.4	25
141	Optical fiber humidity sensor based on a tapered fiber with hydroxyethylcellulose/polyvinylidenefluoride composite. Microwave and Optical Technology Letters, 2014, 56, 380-382.	1.4	25
142	Q-switched ytterbium-doped fiber laser with zinc oxide based saturable absorber. Laser Physics, 2016, 26, 115107.	1.2	25
143	A Microfiber Knot Incorporating a Tungsten Disulfide Saturable Absorber Based Multi-Wavelength Mode-Locked Erbium-Doped Fiber Laser. Journal of Lightwave Technology, 2018, 36, 5633-5639.	4.6	25
144	Nanosecond mode-locked erbium doped fiber laser based on zinc oxide thin film saturable absorber. Indian Journal of Physics, 2019, 93, 93-99.	1.8	25

#	Article	IF	CITATIONS
145	Dark pulse mode-locked fibre laser with zirconia-based erbium-doped fibre (Zr-EDF) and Black phosphorus saturable absorber. Optik, 2020, 223, 165635.	2.9	25
146	Brillouin fiber laser with a 49 cm long Bismuth-based erbium-doped fiber. Laser Physics Letters, 2010, 7, 60-62.	1.4	24
147	Multi-wavelength Brillouin fiber laser using dual-cavity configuration. Laser Physics, 2011, 21, 205-209.	1.2	24
148	Tapered Plastic Optical Fiber Coated With HEC/PVDF for Measurement of Relative Humidity. IEEE Sensors Journal, 2013, 13, 4702-4705.	4.7	24
149	Transition Metal Dichalcogenides (WS ₂ and MoS ₂) Saturable Absorbers for Mode-Locked Erbium-Doped Fiber Lasers. Chinese Physics Letters, 2017, 34, 014202.	3.3	24
150	Lutetium (III) oxide film as passive mode locker device for erbium-doped fibre laser cavity. Optics Communications, 2019, 446, 51-55.	2.1	24
151	Indium Tin Oxide Coated D-Shape Fiber as a Saturable Absorber for Generating a Dark Pulse Mode-Locked Laser*. Chinese Physics Letters, 2020, 37, 054202.	3.3	24
152	Comparisons of multi-wavelength oscillations using Sagnac loop mirror and Mach-Zehnder interferometer for ytterbium doped fiber lasers. Laser Physics, 2010, 20, 516-521.	1.2	23
153	Diode-pumped 1028 nm Ytterbium-doped fiber laser with near 90% slope efficiency. Laser Physics, 2010, 20, 656-660.	1.2	23
154	Visible and near infrared up-conversion luminescence in Yb3+/Tm3+ co-doped yttria-alumino-silicate glass based optical fibers. Journal of Luminescence, 2013, 143, 393-401.	3.1	23
155	Dual-wavelength mode-locked erbium-doped fiber laser based on tin disulfide thin film as saturable absorber. Journal of Applied Physics, 2019, 125, .	2.5	23
156	Lutetium oxide film as a passive saturable absorber for generating Q-switched fiber laser at 1570â€`nm wavelength. Optical Fiber Technology, 2019, 50, 82-86.	2.7	23
157	Optical characterization of different waist diameter on microfiber loop resonator humidity sensor. Sensors and Actuators A: Physical, 2019, 285, 200-209.	4.1	23
158	Indium tin oxide coated D-shape fiber as saturable absorber for passively Q-switched erbium-doped fiber laser. Optics and Laser Technology, 2020, 124, 105998.	4.6	23
159	MAX phase Ti3AlC2 embedded in PVA and deposited onto D-shaped fiber as a passive Q-switcher for erbium-doped fiber laser. Optik, 2020, 224, 165682.	2.9	23
160	Gain enhancement in partial double-pass L-band EDFA system using a band-pass filter. Laser Physics Letters, 2005, 2, 36-38.	1.4	22
161	Double-clad erbium/ytterbium-doped fiber laser with a fiber Bragg grating. Laser Physics Letters, 2009, 6, 586-589.	1.4	22
162	Experimental and theoretical studies on a double-pass C-band bismuth-based erbium-doped fiber amplifier. Optics and Laser Technology, 2010, 42, 790-793.	4.6	22

#	Article	IF	CITATIONS
163	Mode-locked L-band bismuth–erbium fiber laser using carbon nanotubes. Applied Physics B: Lasers and Optics, 2014, 115, 407-412.	2.2	22
164	Performance analysis of an all-optical OFDM system in presence of non-linear phase noise. Optics Express, 2015, 23, 3886.	3.4	22
165	Mechanically exfoliated 2D nanomaterials as saturable absorber for Q-switched erbium doped fiber laser. Indian Journal of Physics, 2017, 91, 1259-1264.	1.8	22
166	EFFECT OF SIZE ON SINGLE AND DOUBLE OPTICAL MICROBOTTLE RESONATOR HUMIDITY SENSORS. Sensors and Actuators A: Physical, 2018, 284, 286-291.	4.1	22
167	Pure gold saturable absorber for generating Q-switching pulses at 2â€ ⁻ µm in Thulium-doped fiber laser cavity. Optical Fiber Technology, 2019, 50, 23-30.	2.7	22
168	Simple design of optical fiber displacement sensor using a multimode fiber coupler. Laser Physics, 2009, 19, 1446-1449.	1.2	21
169	17-channels S band multiwavelength Brillouin/Erbium Fiber Laser co-pump with Raman source. Laser Physics, 2009, 19, 2188-2193.	1.2	21
170	Enhanced bundle fiber displacement sensor based on concave mirror. Sensors and Actuators A: Physical, 2010, 162, 8-12.	4.1	21
171	Dual wavelength erbium-doped fiber laser using a tapered fiber. Journal of Modern Optics, 2010, 57, 2111-2113.	1.3	21
172	Temperature Sensing Using Frequency Beating Technique From Single-Longitudinal Mode Fiber Laser. IEEE Sensors Journal, 2012, 12, 2496-2500.	4.7	21
173	Ultra-narrow linewidth single longitudinal mode Brillouin fiber ring laser using highly nonlinear fiber. Laser Physics Letters, 2013, 10, 105105.	1.4	21
174	Fiber optic displacement sensor for imaging of tooth surface roughness. Measurement: Journal of the International Measurement Confederation, 2013, 46, 546-551.	5.0	21
175	Dumbbell shaped inline Mach–Zehnder interferometer for glucose detection. Measurement: Journal of the International Measurement Confederation, 2015, 59, 167-170.	5.0	21
176	Mode-locked ytterbium-doped fiber laser using mechanically exfoliated black phosphorus as saturable absorber. Optik, 2017, 147, 52-58.	2.9	21
177	An 8â€ [−] cm long holmium-doped fiber saturable absorber for Q-switched fiber laser generation at 2-µm region. Optical Fiber Technology, 2018, 43, 67-71.	2.7	21
178	Mode-Locked YDFL Using Topological Insulator Bismuth Selenide Nanosheets as the Saturable Absorber. Crystals, 2022, 12, 489.	2.2	21
179	Gain Clamping in Two-Stage>tex<\$L\$>/tex<-Band EDFA Using a Broadband FBG. IEEE Photonics Technology Letters, 2004, 16, 422-424.	2.5	20
180	Performance Comparison of Mode-Locked Erbium-Doped Fiber Laser with Nonlinear Polarization Rotation and Saturable Absorber Approaches. Chinese Physics Letters, 2012, 29, 054216.	3.3	20

#	Article	IF	CITATIONS
181	Microfiber Mach-Zehnder interferometer embedded in low index polymer. Optics and Laser Technology, 2012, 44, 1186-1189.	4.6	20
182	A Passively Mode-Locked Erbium-Doped Fiber Laser Based on a Single-Wall Carbon Nanotube Polymer. Chinese Physics Letters, 2013, 30, 054210.	3.3	20
183	Demonstration of side coupling to cladding modes through zinc oxide nanorods grown on multimode optical fiber. Optics Letters, 2013, 38, 3620.	3.3	20
184	Q-switched Yb-doped fiber laser operating at 1073 nm using a carbon nanotubes saturable absorber. Microwave and Optical Technology Letters, 2014, 56, 1770-1773.	1.4	20
185	Tunable dual-wavelength thulium-doped fiber laser at 1.8Âμm region using spatial-mode beating. Journal of Modern Optics, 2015, 62, 892-896.	1.3	20
186	Q-switched ytterbium-doped fiber laser via a thulium-doped fiber saturable absorber. Applied Optics, 2018, 57, 6510.	1.8	20
187	Cobalt oxide nanocubes thin film as saturable absorber for generating Q-switched fiber lasers at 1 and 1.5â€ ⁻ µm in ring cavity configuration. Optical Fiber Technology, 2018, 45, 128-136.	2.7	20
188	Microbottle resonator for formaldehyde liquid sensing. Optik, 2018, 173, 180-184.	2.9	20
189	MXene Ti3C2Tx as a passive Q-switcher for erbium-doped fiber laser. Optical Fiber Technology, 2020, 58, 102289.	2.7	20
190	Ultrafast laser soliton mode-locked at 1.5 \hat{l} /4m region based on Cr2AlC MAX phase as a saturable absorber. Optical Engineering, 2021, 60, .	1.0	20
191	37.2dB small-signal gain from Er/Yb Co-doped fiber amplifier with 20mW pump power. Optics and Laser Technology, 2008, 40, 88-91.	4.6	19
192	The performance of double-clad ytterbium-doped fiber laser with different pumping wavelengths. Laser Physics Letters, 2009, 6, 458-460.	1.4	19
193	Fabrication of tapered fiber based ring resonator. Laser Physics, 2010, 20, 1629-1631.	1.2	19
194	Novel O-band tunable fiber laser using an array waveguide grating. Laser Physics Letters, 2010, 7, 164-167.	1.4	19
195	Wideband Spectrum-Sliced ASE Source Operating at 1900-nm Region Based on a Double-Clad Ytterbium-Sensitized Thulium-Doped Fiber. IEEE Photonics Journal, 2012, 4, 14-18.	2.0	19
196	Self-Starting Harmonic Mode-Locked Thulium-Doped Fiber Laser with Carbon Nanotubes Saturable Absorber. Chinese Physics Letters, 2013, 30, 094204.	3.3	19
197	Circuit Model of Fano Resonance on Tetramers, Pentamers, and Broken Symmetry Pentamers. Plasmonics, 2014, 9, 1303-1313.	3.4	19
198	Enhanced Erbium–Zirconia–Yttria–Aluminum Co-Doped Fiber Amplifier. IEEE Photonics Journal, 2015, 7, 1-7.	2.0	19

#	Article	IF	CITATIONS
199	Q-switched ytterbium-doped fiber laser with topological insulator-based saturable absorber. Optical Engineering, 2017, 56, 056103.	1.0	19
200	Relative humidity sensor employing tapered plastic optical fiber coated with seeded Al-doped ZnO. Optik, 2017, 144, 257-262.	2.9	19
201	Detection of Formaldehyde Vapor Using Glass Substrate Coated With Zinc Oxide Nanorods. IEEE Photonics Journal, 2019, 11, 1-9.	2.0	19
202	Q-Switched YDFL generation by a MAX phase saturable absorber. Applied Optics, 2020, 59, 5408.	1.8	19
203	Estimation of metal surface roughness using fiber optic displacement sensor. Laser Physics, 2010, 20, 904-909.	1.2	18
204	Hybrid flat gain C-band optical amplifier with Zr-based erbium-doped fiber and semiconductor optical amplifier. Laser Physics, 2011, 21, 202-204.	1.2	18
205	A new compact micro-ball lens structure at the cleaved tip of microfiber coupler for displacement sensing. Sensors and Actuators A: Physical, 2013, 189, 177-181.	4.1	18
206	Relative Humidity Sensor Employing Optical Fibers Coated with ZnO Nanostructures. Indian Journal of Science and Technology, 2015, 8, .	0.7	18
207	Generation of switchable domain wall and Cubic–Quintic nonlinear Schrödinger equation dark pulse. Optics and Laser Technology, 2015, 73, 127-129.	4.6	18
208	Passively Q-switched erbium-doped fibre laser using cobalt oxide nanocubes as a saturable absorber. Journal of Modern Optics, 2017, 64, 1315-1320.	1.3	18
209	Quantum dot cadmium selenide as a saturable absorber for Q-switched and mode-locked double-clad ytterbium-doped fiber lasers. Optics Communications, 2017, 397, 147-152.	2.1	18
210	Temperature sensing using CdSe quantum dot doped poly(methyl methacrylate) microfiber. Applied Optics, 2017, 56, 4675.	2.1	18
211	Deposition of silver nanoparticles on polyvinyl alcohol film using electron beam evaporation and its application as a passive saturable absorber. Results in Physics, 2018, 11, 232-236.	4.1	18
212	An efficient wideband hafnia-bismuth erbium co-doped fiber amplifier with flat-gain over 80â€ [–] nm wavelength span. Optical Fiber Technology, 2019, 48, 186-193.	2.7	18
213	Whispering gallery modes on optical micro-bottle resonator for humidity sensor application. Optik, 2019, 185, 558-565.	2.9	18
214	Trisâ€(8â€hydroxyquinoline) aluminium thin film as saturable absorber for passively Qâ€switched erbiumâ€doped fibre laser. IET Optoelectronics, 2019, 13, 247-253.	3.3	18
215	Mechanical exfoliation of indium tin oxide as saturable absorber for Q-switched Ytterbium-doped and Erbium-doped fiber lasers. Optics Communications, 2020, 475, 126217.	2.1	18
216	Tungsten tri-oxide (WO3) film absorber for generating Q-switched pulses in erbium laser. Journal of Modern Optics, 2020, 67, 374-382.	1.3	18

#	Article	IF	CITATIONS
217	Dark pulse emission in nonlinear polarization rotation-based multiwavelength mode-locked erbium-doped fiber laser. Chinese Optics Letters, 2014, 12, 113202-113204.	2.9	18
218	Femtoseconds soliton mode-locked erbium-doped fiber laser based on nickel oxide nanoparticle saturable absorber. Chinese Optics Letters, 2017, 15, 100602.	2.9	18
219	Multiwavelength Laser Comb in L-Band Region with Dual-Cavity Brillouin/Erbium Fiber Laser. Japanese Journal of Applied Physics, 2002, 41, L1234-L1236.	1.5	17
220	Switchable semiconductor optical fiber laser incorporating AWG and broadband FBG with high SMSR. Laser Physics Letters, 2009, 6, 539-543.	1.4	17
221	A simple linear cavity dual-wavelength fiber laser using AWG as wavelength selective mechanism. Laser Physics, 2010, 20, 2006-2010.	1.2	17
222	A compact O-plus C-band switchable quad-wavelength fiber laser using arrayed waveguide grating. Laser Physics Letters, 0, 7, 597-602.	1.4	17
223	Nonlinear Polarization Rotation-Based Mode-Locked Erbium-Doped Fiber Laser with Three Switchable Operation States. Chinese Physics Letters, 2014, 31, 094206.	3.3	17
224	Multi-wavelength Brillouin Raman erbium-doped fiber laser generation in a linear cavity. Journal of Optics (United Kingdom), 2014, 16, 035203.	2.2	17
225	Tunable dual-wavelength ytterbium-doped fiber laser using a strain technique on microfiber Mach–Zehnder interferometer. Applied Optics, 2016, 55, 778.	2.1	17
226	Miniature Compact Folded Dipole for Metal Mountable UHF RFID Tag Antenna. Electronics (Switzerland), 2019, 8, 713.	3.1	17
227	Dissipative soliton generation in Er-doped fibre laser using SnS ₂ as a saturable absorber. Applied Physics Express, 2019, 12, 102008.	2.4	17
228	Poly(3-hexylthiophene-2,5-diyl) regioregular (P3HT) thin film as saturable absorber for passively Q-switched and mode-locked Erbium-doped fiber laser. Optical Fiber Technology, 2020, 54, 102073.	2.7	17
229	Power-dependent nonlinear optical behaviours of ponceau BS chromophore at 532 nm via Z-scan technique. Journal of Photochemistry and Photobiology A: Chemistry, 2020, 397, 112574.	3.9	17
230	Single-Mode Modified Tapered Fiber Structure Functionalized With GO-PVA Composite Layer for Relative Humidity Sensing. Photonic Sensors, 2021, 11, 314-324.	5.0	17
231	High-energy Q-switched ytterbium-doped all-fiber laser with tris-(8-hydroxyquinoline) aluminum as saturable absorber. Optical Materials Express, 2019, 9, 3215.	3.0	17
232	BRILLOUIN FIBER LASER WITH SIGNIFICANTLY REDUCED GAIN MEDIUM LENGTH OPERATING IN L-BAND REGION. Progress in Electromagnetics Research Letters, 2009, 8, 143-149.	0.7	17
233	Fiber-optic displacement sensor using a multimode bundle fiber. Microwave and Optical Technology Letters, 2008, 50, 661-663.	1.4	16
234	Brillouin fibre laser with 20â€m-long photonic crystal fibre. Electronics Letters, 2008, 44, 1065.	1.0	16

#	Article	IF	CITATIONS
235	OPTIMIZATION OF THE 1050nm PUMP POWER AND FIBER LENGTH IN SINGLE-PASS AND DOUBLE-PASS THULIUM DOPED FIBER AMPLIFIERS. Progress in Electromagnetics Research B, 2009, 14, 431-448.	1.0	16
236	Compact Brillouin Fiber Laser Based on Highly Nonlinear Fiber With 51 Double Spacing Channels. IEEE Photonics Journal, 2012, 4, 1087-1094.	2.0	16
237	Regenerated fibre Bragg grating fabricated on high germanium concentration photosensitive fibre for sensing at high temperature. Optics and Laser Technology, 2012, 44, 821-824.	4.6	16
238	Mode-locked thulium–bismuth codoped fiber laser using graphene saturable absorber in ring cavity. Applied Optics, 2013, 52, 1226.	1.8	16
239	Multiwall carbon nanotube polyvinyl alcohol-based saturable absorber in passively Q-switched fiber laser. Applied Optics, 2014, 53, 7025.	1.8	16
240	Multi-wavelength Q-switched Erbium-doped fiber laser with photonic crystal fiber and multi-walled carbon nanotubes. Journal of Modern Optics, 2014, 61, 1133-1139.	1.3	16
241	Passively dual-wavelength Q-switched ytterbium doped fiber laser using Selenium Bismuth as saturable absorber. Journal of Modern Optics, 2015, 62, 1550-1554.	1.3	16
242	Performance comparison of enhanced Erbium–Zirconia–Yttria–Aluminum co-doped conventional erbium-doped fiber amplifiers. Optik, 2017, 132, 75-79.	2.9	16
243	Formaldehyde sensing using ZnO nanorods coated glass integrated with microfiber. Optics and Laser Technology, 2019, 120, 105750.	4.6	16
244	Mode-locked thulium doped fibre laser with copper thin film saturable absorber. Journal of Modern Optics, 2019, 66, 1381-1385.	1.3	16
245	NiS2 as a broadband saturable absorber for ultrafast pulse lasers. Optics and Laser Technology, 2020, 132, 106492.	4.6	16
246	Passively mode-locked laser at 1μm region based on tungsten trioxide (WO3) saturable absorber. Optik, 2021, 231, 166377.	2.9	16
247	Dual-stage Er/Yb doped fiber amplifier for gain and noise figure enhancements. IEICE Electronics Express, 2006, 3, 517-521.	0.8	15
248	Gain and noise figure improvements in a shorter wavelength region of EDFA using a macrobending approach. Laser Physics, 2008, 18, 1362-1364.	1.2	15
249	Analytical and experimental studies on asymmetric bundle fiber displacement sensors. Journal of Modern Optics, 2009, 56, 1838-1842.	1.3	15
250	Multi-wavelength laser generation with Bismuthbased Erbium-doped fiber. Optics Express, 2009, 17, 203.	3.4	15
251	High output power Erbium-Ytterbium doped cladding pumped fiber amplifier. Laser Physics, 2010, 20, 1899-1901.	1.2	15
252	Fabrication and application of zirconia-erbium doped fibers. Optical Materials Express, 2012, 2, 1690.	3.0	15

#	Article	IF	CITATIONS
253	Tunable single longitudinal mode S-band fiber laser using a 3 m length of erbium-doped fiber. Journal of Modern Optics, 2012, 59, 268-273.	1.3	15
254	Supercontinuum from Zr-EDF using Zr-EDF mode-locked fiber laser. Laser Physics Letters, 2012, 9, 44-49.	1.4	15
255	Thermal Regeneration in Etched-Core Fiber Bragg Grating. IEEE Sensors Journal, 2013, 13, 2581-2585.	4.7	15
256	Fiber optic salinity sensor using beam-through technique. Optik, 2013, 124, 679-681.	2.9	15
257	Q-Switching Pulse Generation with Thulium-Doped Fiber Saturable Absorber. Chinese Physics Letters, 2014, 31, 124203.	3.3	15
258	Fabrication of polymer microfiber by direct drawing. Microwave and Optical Technology Letters, 2015, 57, 820-823.	1.4	15
259	A passively Q-switched ytterbium-doped fiber laser based on a few-layer Bi ₂ Se ₃ saturable absorber. Laser Physics, 2015, 25, 065102.	1.2	15
260	Holmium Oxide Film as a Saturable Absorber for 2 μ m Q-Switched Fiber Laser. Chinese Physics Letters, 2017, 34, 054201.	3.3	15
261	Polyaniline-Doped Poly (Methyl Methacrylate) Microfiber for Methanol Sensing. IEEE Sensors Journal, 2018, 18, 2801-2806.	4.7	15
262	Molybdenum disulfide saturable absorber for eye-safe mode-locked fiber laser generation. Journal of Nonlinear Optical Physics and Materials, 2018, 27, 1850010.	1.8	15
263	Q-switched Ytterbium doped fibre laser using gold nanoparticles saturable absorber fabricated by electron beam deposition. Optik, 2019, 182, 241-248.	2.9	15
264	Soliton mode-locked Er-doped fiber laser by using Alq3 saturable absorber. Optics and Laser Technology, 2020, 123, 105893.	4.6	15
265	Enhanced triple-pass hybrid erbium doped fiber amplifier using distribution pumping scheme in a dual-stage configuration. Optik, 2020, 204, 164191.	2.9	15
266	Mode-locked erbium-doped fiber laser via evanescent field interaction with indium tin oxide. Optical Fiber Technology, 2020, 55, 102124.	2.7	15
267	Q-switched and mode-locked erbium-doped fiber laser using gadolinium oxide as saturable absorber. Optical Fiber Technology, 2020, 57, 102209.	2.7	15
268	Aluminium zinc oxide as a saturable absorber for passively Q-switched and mode-locked erbium-doped fiber laser. Laser Physics, 2021, 31, 055101.	1.2	15
269	Gain Control in L-Band Erbium-Doped Fiber Amplifier Using a Ring Resonator. Japanese Journal of Applied Physics, 2002, 41, L332-L333.	1.5	14
270	Bismuth-based Brillouin/erbium fiber laser. Journal of Modern Optics, 2008, 55, 1345-1351.	1.3	14

#	Article	IF	CITATIONS
271	Lateral and axial displacements measurement using fiber optic sensor based on beamâ€through technique. Microwave and Optical Technology Letters, 2009, 51, 2038-2040.	1.4	14
272	Tunable laser generation with erbium-doped microfiber knot resonator. Laser Physics, 2012, 22, 588-591.	1.2	14
273	Multi-wavelength Brillouin–Raman fiber laser generation assisted by multiple four-wave mixing processes in a ring cavity. Laser Physics, 2013, 23, 075108.	1.2	14
274	Proposal and Performance Evaluation of an Efficient RZ-DQPSK Modulation Scheme in All-Optical OFDM Transmission Systems. Journal of Optical Communications and Networking, 2013, 5, 932.	4.8	14
275	Mode-locking pulse generation with MoS_2–PVA saturable absorber in both anomalous and ultra-long normal dispersion regimes. Applied Optics, 2016, 55, 4247.	2.1	14
276	Side coupling of multiple optical channels by spiral patterned zinc oxide coatings on large core plastic optical fibers. Micro and Nano Letters, 2016, 11, 122-126.	1.3	14
277	Single-mode D-shaped optical fiber sensor for the refractive index monitoring of liquid. Journal of Modern Optics, 2016, 63, 750-755.	1.3	14
278	Optical Microfiber Sensing of Adulterated Honey. IEEE Sensors Journal, 2017, 17, 5510-5514.	4.7	14
279	Compact and flat-gain fiber optical amplifier with Hafnia-Bismuth-Erbium co-doped fiber. Optik, 2018, 170, 56-60.	2.9	14
280	Nanosecond Pulse Generation with Silver Nanoparticle Saturable Absorber*. Chinese Physics Letters, 2019, 36, 054202.	3.3	14
281	Sodium nitrate (NaNO3) sensor based on graphene coated microfiber. Measurement: Journal of the International Measurement Confederation, 2019, 146, 208-214.	5.0	14
282	Wideband and flat gain series erbium doped fiber amplifier using hybrid active fiber with backward pumping distribution technique. Results in Physics, 2019, 13, 102186.	4.1	14
283	Multimode interference based fiber-optic sensor for temperature measurement. Journal of Physics: Conference Series, 2019, 1151, 012023.	0.4	14
284	All fiber multiwavelength Tm-doped double-clad fiber laser assisted by four-wave mixing in highly nonlinear fiber and Sagnac loop mirror. Optics Communications, 2020, 456, 124589.	2.1	14
285	Passively Q-switched erbium-doped fiber laser with mechanical exfoliation of 8-HQCDCL2H2O as saturable absorber. Optik, 2021, 242, 167073.	2.9	14
286	Nanosecond passively Q-switched fibre laser using a NiS2 based saturable absorber. Optics Express, 2019, 27, 19843.	3.4	14
287	Generation of Kelly and dip type sidebands soliton employing Topological insulator (Bi2Te3) as saturable absorber. Infrared Physics and Technology, 2022, 123, 104154.	2.9	14
288	Efficient multiwavelength generation of Brillouin/erbium fiber laser at 1600-nm region. Microwave and Optical Technology Letters, 2002, 35, 506-508.	1.4	13

#	Article	IF	CITATIONS
289	Low noise double pass L-band erbium-doped fiber amplifier. Optics and Laser Technology, 2004, 36, 245-248.	4.6	13
290	Effects of different Raman pumping schemes on stimulated Brillouin scattering in a linear cavity. Applied Optics, 2008, 47, 3088.	2.1	13
291	Multiwavelength ytterbiumâ€doped fiber ring laser. Microwave and Optical Technology Letters, 2009, 51, 2511-2512.	1.4	13
292	Compact Bi-EDF-Based Brillouin Erbium Fiber Laser Operating at the 1560-nm Region. IEEE Photonics Journal, 2009, 1, 254-258.	2.0	13
293	Linear all-fiber temperature sensor based on macro-bent erbium doped fiber. Laser Physics Letters, 2010, 7, 739-742.	1.4	13
294	S-band multiwavelength Brillouin Raman Fiber Laser. Optics Communications, 2011, 284, 4971-4974.	2.1	13
295	Gain-flattened S-band depressed cladding erbium doped fiber amplifier with a flat bandwidth of 12 nm using a Tunable Mach-Zehnder Filter. Laser Physics, 2011, 21, 1633-1637.	1.2	13
296	Double-pass erbium-doped zirconia fiber amplifier for wide-band and flat-gain operations. Optics and Laser Technology, 2011, 43, 1279-1281.	4.6	13
297	Analytical Model for Broadband Thulium-Bismuth-Doped Fiber Amplifier. IEEE Journal of Quantum Electronics, 2012, 48, 1052-1058.	1.9	13
298	Graphene Oxide-Based Q -Switched Erbium-Doped Fiber Laser. Chinese Physics Letters, 2013, 30, 024208.	3.3	13
299	Highly stable graphene-assisted tunable dual-wavelength erbium-doped fiber laser. Applied Optics, 2013, 52, 818.	1.8	13
300	Demonstration of acoustic vibration sensor based on microfiber knot resonator. Microwave and Optical Technology Letters, 2013, 55, 1138-1141.	1.4	13
301	Passively Q-Switched EDFL Using a Multi-Walled Carbon Nanotube Polymer Composite Based on a Saturable Absorber. Chinese Physics Letters, 2014, 31, 034204.	3.3	13
302	Molybdenum Disulphide Tape Saturable Absorber for Mode-Locked Double-Clad Ytterbium-Doped All-Fiber Laser Generation. Chinese Physics Letters, 2016, 33, 114201.	3.3	13
303	Steel Beam Compressive Strain Sensor Using Single-Mode-Multimode-Single-Mode Fiber Structure. IEEE Photonics Journal, 2016, 8, 1-6.	2.0	13
304	Potassium permanganate (KMnO_4) sensing based on microfiber sensors. Applied Optics, 2017, 56, 224.	2.1	13
305	Optical dynamic range maximization for humidity sensing by controlling growth of zinc oxide nanorods. Photonics and Nanostructures - Fundamentals and Applications, 2018, 30, 57-64.	2.0	13
306	Nickel oxide nanoparticles thin film saturable absorber for 1-micron pulsed all-fibre lasers operation. Journal of Modern Optics, 2018, 65, 1801-1808.	1.3	13

#	Article	IF	CITATIONS
307	Qâ€switched and mode″ocked ytterbiumâ€doped fibre lasers with Sb 2 Te 3 topological insulator saturable absorber. IET Optoelectronics, 2018, 12, 180-184.	3.3	13
308	Microfiber loop resonator for formaldehyde liquid sensing. Optik, 2019, 196, 163174.	2.9	13
309	Femtosecond mode-locked laser at 1.5Âμm region using turmeric-based saturable absorber. Infrared Physics and Technology, 2020, 111, 103548.	2.9	13
310	Ultrashort pulse generation with MXene Ti3C2Tx embedded in PVA and deposited onto D-shaped fiber. Optics and Laser Technology, 2021, 136, 106780.	4.6	13
311	Soliton mode-locked pulse generation with a bulk structured MXene Ti ₃ AlC ₂ deposited onto a D-shaped fiber. Applied Optics, 2020, 59, 8759.	1.8	13
312	A Review: Surface Plasmon Resonance-Based Biosensor for Early Screening of SARS-CoV2 Infection. IEEE Access, 2022, 10, 1228-1244.	4.2	13
313	L-band erbium-doped fibre amplifier with clamped- and flattened-gain using FBG. Electronics Letters, 2003, 39, 1238.	1.0	12
314	Self-Calibrating Automated Characterization System for Depressed Cladding EDFA Applications Using LabVIEW Software With GPIB. IEEE Transactions on Instrumentation and Measurement, 2008, 57, 2677-2681.	4.7	12
315	Tunable high power fiber laser using an AWG as the tuning element. Laser Physics, 2011, 21, 712-717.	1.2	12
316	Environmentâ€independent liquid level sensing based on fiberâ€optic displacement sensors. Microwave and Optical Technology Letters, 2011, 53, 2451-2453.	1.4	12
317	New Design of a Thulium–Aluminum-Doped Fiber Amplifier Based on Macro-Bending Approach. Journal of Lightwave Technology, 2012, 30, 3263-3272.	4.6	12
318	Stable double spacing multiwavelength Brillouin-Erbium doped fiber laser based on highly nonlinear fiber. Laser Physics, 2012, 22, 977-981.	1.2	12
319	Fiber laser at 2 micron region using double-clad thulium/ytterbium co-doped yttria-alumino-silicate fiber. Laser Physics Letters, 2012, 9, 50-53.	1.4	12
320	Passively mode-locked erbium doped zirconia fiber laser using a nonlinear polarisation rotation technique. Optics and Laser Technology, 2013, 47, 22-25.	4.6	12
321	Passive Q-switched Erbium-doped fiber laser with graphene–polyethylene oxide saturable absorber in three different gain media. Indian Journal of Physics, 2014, 88, 727-731.	1.8	12
322	<scp>PMMA</scp> microfiber coated with alâ€doped ZnO nanostructures for detecting uric acid. Microwave and Optical Technology Letters, 2015, 57, 2455-2457.	1.4	12
323	Single mode EDF fiber laser using an ultra-narrow bandwidth tunable optical filter. Optik, 2015, 126, 179-183.	2.9	12
324	Applied light-side coupling with optimized spiral-patterned zinc oxide nanorod coatings for multiple optical channel alcohol vapor sensing. Journal of Nanophotonics, 2016, 10, 036009.	1.0	12

#	Article	IF	CITATIONS
325	Q-switched erbium-doped fiber laser operating at 1502nm with molybdenum disulfide saturable absorber. Journal of Nonlinear Optical Physics and Materials, 2016, 25, 1650025.	1.8	12
326	Multi-Wavelength Q-Switched Ytterbium-Doped Fiber Laser with Multi-Walled Carbon Nanotubes. Fiber and Integrated Optics, 2018, 37, 92-102.	2.5	12
327	Short-pulsed Q-switched Thulium doped fiber laser with graphene oxide as a saturable absorber. Optik, 2018, 168, 462-466.	2.9	12
328	Nickel oxide film saturable absorber for mode-locking operation at 1.55-micron region. Journal of Nonlinear Optical Physics and Materials, 2018, 27, 1850020.	1.8	12
329	Theoretical and experimental studies on a Q-switching operation in an erbium-doped fiber laser using vanadium oxide as saturable absorber. Laser Physics, 2018, 28, 085106.	1.2	12
330	PAPR reduction in all-optical OFDM based on time interleaving odd and even subcarriers. Optics Communications, 2019, 437, 237-245.	2.1	12
331	Low-Cost Integrated Zinc Oxide Nanorod-Based Humidity Sensors for Arduino Platform. IEEE Sensors Journal, 2019, 19, 2442-2449.	4.7	12
332	ZnO nanorod-coated tapered plastic fiber sensors for relative humidity. Optics Communications, 2020, 473, 125924.	2.1	12
333	Nanosecond passively Q-switched fiber laser in the 1.5µm region using turmeric saturable absorber. Optics and Laser Technology, 2021, 139, 106971.	4.6	12
334	Gainâ€flattened hybrid EDFA operating in C + L band with parallel pumping distribution technique. IET Optoelectronics, 2020, 14, 447-451.	3.3	12
335	Optical Humidity Sensor Based on Tapered Fiber with Multi-walled Carbon Nanotubes Slurry. Indonesian Journal of Electrical Engineering and Computer Science, 2017, 6, 97.	0.8	12
336	1028 nm single mode Ytterbium-doped fiber laser. Laser Physics, 2009, 19, 1021-1025.	1.2	11
337	Compact and Tunable Erbium-Doped Fiber Laser With Microfiber Mach–Zehnder Interferometer. IEEE Journal of Quantum Electronics, 2012, 48, 1165-1168.	1.9	11
338	Add-Drop Filter Based on Microfiber Mach–Zehnder/Sagnac Interferometer. IEEE Journal of Quantum Electronics, 2012, 48, 1411-1414.	1.9	11
339	Upconversion luminescence in Tm ³⁺ /Yb ³⁺ co-doped double-clad silica fibers under 980 nm cladding pumping. Journal of Modern Optics, 2012, 59, 527-532.	1.3	11
340	A <i>Q</i> -switched multi-wavelength Brillouin erbium fiber laser with a single-walled carbon nanotube saturable absorber. Laser Physics, 2013, 23, 055101.	1.2	11
341	Wideband tunable Q-switched fiber laser using graphene as a saturable absorber. Journal of Modern Optics, 2013, 60, 1563-1568.	1.3	11
342	Fiber Optic Displacement Sensor Using Multimode Plastic Fiber Probe and Tooth Surface. IEEE Sensors Journal, 2013, 13, 294-298.	4.7	11

#	Article	IF	CITATIONS
343	Tunable, low frequency microwave generation from AWG based closely-spaced dual-wavelength single-longitudinal-mode fibre laser. Journal of the European Optical Society-Rapid Publications, 0, 8, .	1.9	11
344	Stable narrow spacing dual-wavelength Q-switched graphene oxide embedded in a photonic crystal fiber. Laser Physics, 2014, 24, 105101.	1.2	11
345	A tuneable, power efficient and narrow single longitudinal mode fibre ring laser using an inline dual-taper fibre Mach–Zehnder filter. Laser Physics, 2014, 24, 085111.	1.2	11
346	Low-Cost Transducer Based On Surface Scattering Using Side-Polished D-Shaped Optical Fibers. IEEE Photonics Journal, 2015, 7, 1-10.	2.0	11
347	Tapered fiber coated with hydroxyethyl cellulose/polyvinylidene fluoride composite for relative humidity sensor. Sensors and Actuators A: Physical, 2015, 225, 128-132.	4.1	11
348	Mitigation of phase noise in all-optical OFDM systems based on minimizing interaction time between subcarriers. Optics Communications, 2015, 355, 313-320.	2.1	11
349	Tunable passively Q-switched thulium-doped fiber laser operating at 1.9 μm using arrayed waveguide grating (AWG). Optics Communications, 2016, 380, 195-200.	2.1	11
350	Effects of the Dopant Ratio on Polyaniline Coated Fiber Bragg Grating for pH detection. Synthetic Metals, 2016, 211, 132-141.	3.9	11
351	Experimental Observation of Bright and Dark Solitons Mode-Locked with Zirconia-Based Erbium-Doped Fiber Laser. Chinese Physics Letters, 2018, 35, 024203.	3.3	11
352	Flat-gain and wide-band partial double-pass erbium co-doped fiber amplifier with hybrid gain medium. Optical Fiber Technology, 2019, 52, 101952.	2.7	11
353	Q-switched and tunable wavelength fiber laser utilizing nickel oxide saturable absorber and sagnac loop mirror filter. Infrared Physics and Technology, 2020, 109, 103433.	2.9	11
354	Humidity sensing using microfiber-ZnO nanorods coated glass structure. Optik, 2021, 238, 166715.	2.9	11
355	Ti3AlC2 MAX phase thin film as saturable absorber for generating soliton mode-locked fiber laser. Optik, 2021, 245, 167767.	2.9	11
356	Q-switched Erbium-doped Fiber Laser with a Black Phosphorus Saturable Absorber. Photonics Letters of Poland, 2017, 9, 72.	0.4	11
357	Generation of passively Qâ€switched ytterbium laser by using tungsten triâ€oxide film absorber. IET Optoelectronics, 2020, 14, 278-284.	3.3	11
358	Effect of doped-fiber's spooling on performance of S-band EDFA. Laser Physics Letters, 2005, 2, 412-414.	1.4	10
359	A linear cavity brillouin/bismuth-based erbium-doped fiber laser with enhanced characteristics. Laser Physics, 2008, 18, 1344-1348.	1.2	10
360	Flat output and switchable fiber laser using AWG and broadband FBG. Optics Communications, 2009, 282, 2576-2579.	2.1	10

#	Article	IF	CITATIONS
361	Dual-Wavelength Erbium Fiber Laser in a Simple Ring Cavity. Fiber and Integrated Optics, 2009, 28, 430-439.	2.5	10
362	\$O\$-Band Bismuth-Doped Fiber Amplifier With Double-Pass Configuration. IEEE Photonics Technology Letters, 2011, 23, 1860-1862.	2.5	10
363	Compact fiber laser at L-band region using Erbium-doped Zirconia fiber. Laser Physics, 2011, 21, 176-179.	1.2	10
364	Flat and compact switchable dual wavelength output at 1060nm from ytterbium doped fiber laser with an AWG as a wavelength selector. Optics and Laser Technology, 2011, 43, 550-554.	4.6	10
365	Non-membrane optical microphone based on longitudinal modes competition. Sensors and Actuators A: Physical, 2011, 168, 281-285.	4.1	10
366	56 dB Gain EYDFA with improved noise figure with dual-stage partial double pass configuration. Optik, 2012, 123, 1884-1887.	2.9	10
367	Performance evaluation of a bilayer SPR-based fiber optic RI sensor with TiO2 using FDTD solutions. Photonic Sensors, 2014, 4, 289-294.	5.0	10
368	Introduction to the Issue on Fiber Lasers. IEEE Journal of Selected Topics in Quantum Electronics, 2014, 20, 5-7.	2.9	10
369	Multi-wavelength Q-switched Erbium-doped fiber laser with photonic crystal fiber and graphene – Polyethylene oxide saturable absorber. Optik, 2015, 126, 1495-1498.	2.9	10
370	Q-Switched Raman Fiber Laser with Molybdenum Disulfide-Based Passive Saturable Absorber. Chinese Physics Letters, 2016, 33, 074208.	3.3	10
371	Light backscattering (e.g. reflectance) by ZnO nanorods on tips of plastic optical fibres with application for humidity and alcohol vapour sensing. Micro and Nano Letters, 2016, 11, 832-836.	1.3	10
372	Switchable soliton mode-locked and multi-wavelength operation in thulium-doped all-fiber ring laser. Journal of Nonlinear Optical Physics and Materials, 2016, 25, 1650034.	1.8	10
373	Broadband tuning in a passively Q-switched erbium doped fiber laser (EDFL) via multiwall carbon nanotubes/polyvinyl alcohol (MWCNT/PVA) saturable absorber. Optics Communications, 2016, 365, 54-60.	2.1	10
374	Stretched and soliton femtosecond pulse generation with graphene saturable absorber by manipulating cavity dispersion. Optik, 2017, 138, 250-255.	2.9	10
375	Cadmium Selenide Polymer Microfiber Saturable Absorber for Q-Switched Fiber Laser Applications. Chinese Physics Letters, 2017, 34, 094202.	3.3	10
376	Gold nanoparticle based saturable absorber for Q-switching in 1.5 <i>µ</i> m laser application. Laser Physics, 2017, 27, 115101.	1.2	10
377	Graphene coated silica microfiber for highly sensitive magnesium sensor. Sensors and Actuators A: Physical, 2018, 273, 67-71.	4.1	10
378	Q-Switched Erbium-Doped Fiber Laser Using Cadmium Selenide Coated onto Side-Polished D-Shape Fiber as Saturable Absorber. Chinese Physics Letters, 2018, 35, 104201.	3.3	10

#	Article	IF	CITATIONS
379	Wideband optical fiber amplifier with short length of enhanced erbium–zirconia–yttria–aluminum co-doped fiber. Optik, 2019, 182, 194-200.	2.9	10
380	Effect of PMMA and PVA coating on the performance of optical microbottle resonator humidity sensors. Microwave and Optical Technology Letters, 2020, 62, 993-998.	1.4	10
381	U-Shaped Inductively Coupled Feed UHF RFID Tag Antenna With DMS for Metal Objects. IEEE Antennas and Wireless Propagation Letters, 2020, 19, 907-911.	4.0	10
382	Mode-locked laser at 1066 nm by using Alq3 as saturable absorber in all-fiber based cavity. Optik, 2020, 219, 165179.	2.9	10
383	ZnO nanorods coated microfiber loop resonator for relative humidity sensing. Optical Fiber Technology, 2020, 54, 102080.	2.7	10
384	Q-switched and mode-locked laser based on aluminium zinc oxide deposited onto D-shape fiber as a saturable absorber. Results in Optics, 2021, 3, 100057.	2.0	10
385	Formaldehyde sensor with enhanced performance using microsphere resonator-coupled ZnO nanorods coated glass. Optics and Laser Technology, 2021, 139, 106853.	4.6	10
386	Titanium dioxide fiber saturable absorber for Q-switched fiber laser generation in the 1-micrometer region. Applied Optics, 2019, 58, 3495.	1.8	10
387	Sideband-controllable soliton pulse with bismuth-based erbium-doped fiber. Chinese Optics Letters, 2015, 13, 111406-111408.	2.9	10
388	New Brillouin fiber laser configuration with high output power. Microwave and Optical Technology Letters, 2007, 49, 2656-2658.	1.4	9
389	Gain and noise figure improvements in double-pass S-band EDFA. Optics and Laser Technology, 2007, 39, 935-938.	4.6	9
390	High-power single-wavelength SOA-based fiber-ring laser with an optical modulator. Laser Physics, 2008, 18, 1349-1352.	1.2	9
391	FIBER LOOP MIRROR FILTER WITH TWO-STAGE HIGH BIREFRINGENCE FIBERS. Progress in Electromagnetics Research C, 2009, 9, 101-108.	0.9	9
392	L-BAND AMPLIFICATION AND MULTI-WAVELENGTH LASING WITH BISMUTH-BASED ERBIUM DOPED FIBER. Progress in Electromagnetics Research C, 2009, 6, 1-12.	0.9	9
393	Displacement sensing with two asymmetrical inclined fibers. Microwave and Optical Technology Letters, 2010, 52, 1271-1274.	1.4	9
394	67 cm long bismuth-based erbium doped fiber amplifier with wideband operation. Laser Physics Letters, 2011, 8, 814-817.	1.4	9
395	Micro-bending based optical band-pass filter and its application in S-band Thulium-doped fiber amplifier. Optics Express, 2012, 20, 29784.	3.4	9
396	Study of Dual-Wavelength Mode Competition in an Erbium-Doped Fiber Laser (EDFL) Produced by Acoustic Waves. IEEE Journal of Quantum Electronics, 2012, 48, 1499-1504.	1.9	9

#	Article	IF	CITATIONS
397	Alloying aluminum with Fe using laser induced plasma technique. Laser Physics, 2012, 22, 1364-1367.	1.2	9
398	All fiber passively mode locked zirconium-based erbium-doped fiber laser. Optics and Laser Technology, 2012, 44, 534-537.	4.6	9
399	Multi-wavelength fiber laser based on nonlinear polarization rotation in semiconductor optical amplifier and photonic crystal fiber. Laser Physics, 2012, 22, 1257-1259.	1.2	9
400	A Multi-Wavelength Brillouin Erbium Fiber Laser With Double Brillouin Frequency Spacing and Q-Switching Characteristics. IEEE Journal of Quantum Electronics, 2013, 49, 595-598.	1.9	9
401	A Polyaniline-Coated Integrated Microfiber Resonator for UV Detection. IEEE Sensors Journal, 2013, 13, 2020-2025.	4.7	9
402	Temperature Compensation in Determining of Remazol Black B Concentrations Using Plastic Optical Fiber Based Sensor. Sensors, 2014, 14, 15836-15848.	3.8	9
403	Excitation of core modes through side coupling to multimode optical fiber by hydrothermal growth of ZnO nanorods for wide angle optical reception. Journal of the Optical Society of America B: Optical Physics, 2014, 31, 2232.	2.1	9
404	Evanescent wave optical trapping and transport of polystyrene microspheres on microfibers. Microwave and Optical Technology Letters, 2014, 56, 2630-2634.	1.4	9
405	Tapered plastic optical fiber coated with single wall carbon nanotubes polyethylene oxide composite for measurement of uric acid concentration. Sensor Review, 2014, 34, 75-79.	1.8	9
406	Soliton Mode-Locked Erbium-Doped Fiber Laser Using Non-Conductive Graphene Oxide Paper. IEEE Journal of Quantum Electronics, 2014, 50, 85-87.	1.9	9
407	Tunable microwave output over a wide RF region generated by an optical dual-wavelength fiber laser. Laser Physics, 2014, 24, 105116.	1.2	9
408	Peak-to-average power ratio reduction in all-optical orthogonal frequency division multiplexing system using rotated constellation approach. Optical Fiber Technology, 2015, 25, 88-93.	2.7	9
409	Dual wavelength single longitudinal mode Ytterbium-doped fiber laser using a dual-tapered Mach-Zehnder interferometer. Journal of the European Optical Society-Rapid Publications, 0, 10, .	1.9	9
410	Fabrication and Characterization of a Refractive Index Sensor Based on SPR in an Etched Plastic Optical Fiber. Procedia Engineering, 2015, 120, 969-974.	1.2	9
411	Inline Mach–Zehnder interferometer with ZnO nanowires coating for the measurement of uric acid concentrations. Sensors and Actuators A: Physical, 2015, 234, 206-211.	4.1	9
412	Effectiveness of phase-conjugated twin waves on fiber nonlinearity in spatially multiplexed all-optical OFDM system. Optical Fiber Technology, 2016, 30, 147-152.	2.7	9
413	Fabrication and characterization of high order filter based on resonance in hybrid multi-knots microfiber structure. Optics and Laser Technology, 2016, 78, 120-124.	4.6	9
414	Passively Q-switched flashlamp pumped Nd:YAG laser using liquid graphene oxide as saturable absorber. Optics and Laser Technology, 2016, 80, 28-32.	4.6	9

#	Article	IF	CITATIONS
415	Bi ₂ Te ₃ based passively Q-switched at 1042.76 and 1047 nm wavelength. Laser Physics, 2017, 27, 125102.	1.2	9
416	A Flat-Gain Double-Pass Amplifier with New Hafnia-Bismuth-Erbium Codoped Fiber. Chinese Physics Letters, 2018, 35, 054206.	3.3	9
417	Microbottle resonator for temperature sensing. Journal of Physics: Conference Series, 2019, 1371, 012006.	0.4	9
418	Q-switched erbium-doped fiber laser with silicon oxycarbide saturable absorber. Optik, 2020, 219, 165234.	2.9	9
419	Mode-locked operation with 9kW peak power using Au nanoparticles saturable absorber. Optik, 2021, 227, 165976.	2.9	9
420	Ultra-short pulse generating in erbium-doped fiber laser cavity with 8-Hydroxyquinolino cadmium chloride hydrate (8-HQCdCl ₂ H ₂ O) saturable absorber. Journal of Modern Optics, 2021, 68, 237-245.	1.3	9
421	Integrating microsphere resonator and ZnO nanorods coated glass for humidity sensing application. Optics and Laser Technology, 2021, 143, 107356.	4.6	9
422	Passively Q-switched pulses from ytterbium-doped fiber laser (YDFL) using copper oxide (CuO) nanoparticles as a saturable absorber. Optical Materials Express, 2020, 10, 2896.	3.0	9
423	Ytterbium-sensitized thulium-doped f iber laser with a single-mode output operating at 1 900-nm region. Chinese Optics Letters, 2012, 10, 101401-101403.	2.9	9
424	Chromium aluminum carbide as Q-switcher for the near-infrared erbium-doped fiber laser. Optik, 2022, 250, 168362.	2.9	9
425	Gain improvement in L-band EDFA using unpumped EDF in a double pass system. Microwave and Optical Technology Letters, 2003, 36, 154-156.	1.4	8
426	Design and Operation of a Concentric-Fiber Displacement Sensor. Fiber and Integrated Optics, 2009, 28, 301-309.	2.5	8
427	Bismuth erbium-doped fiber based multi-wavelength laser assisted by four-wave mixing process. IEICE Electronics Express, 2009, 6, 40-43.	0.8	8
428	Performance comparison between plastic-based fiber bundle and multimode fused coupler as probes in displacement sensors. Laser Physics, 2010, 20, 1890-1893.	1.2	8
429	Semiconductor optical amplifier-based multi-wavelength ring laser utilizing photonic crystal fiber. Journal of Modern Optics, 2010, 57, 637-640.	1.3	8
430	Theoretical and experimental studies on concave mirrorâ€based fiber optic displacement sensor. Sensor Review, 2011, 31, 65-69.	1.8	8
431	DC current sensing capability of microfibre Mach-Zehnder interferometer. Electronics Letters, 2012, 48, 943.	1.0	8
432	Microfibre Mach–Zehnder interferometer and its application as a current sensor. IET Optoelectronics, 2012, 6, 298-302.	3.3	8

#	Article	IF	CITATIONS
433	Tunable Radio Frequency Generation Using a Graphene-Based Single Longitudinal Mode Fiber Laser. Journal of Lightwave Technology, 2012, 30, 2097-2102.	4.6	8
434	Demonstration of microfiber hybrid Mach–Zehnder and knot resonator structure. Microwave and Optical Technology Letters, 2013, 55, 100-102.	1.4	8
435	S-band multiwavelength Brillouin/Raman distributed Bragg reflector fiber lasers. Applied Optics, 2013, 52, 3753.	1.8	8
436	Mode-locked soliton erbium-doped fiber laser using a single-walled carbon nanotubes embedded in polyethylene oxide thin film saturable absorber. Journal of Modern Optics, 2014, 61, 541-545.	1.3	8
437	Qâ€switched thuliumâ€doped fiber laser operating at 1920 nm region with multiwalled carbon nanotubes embedded in polyvinyl alcohol. Microwave and Optical Technology Letters, 2014, 56, 2817-2819.	1.4	8
438	Mode-Locked Thulium Ytterbium Co-Doped Fiber Laser with Graphene Oxide Paper Saturable Absorber. Chinese Physics Letters, 2015, 32, 014204.	3.3	8
439	Multi-lobed double-clad Erbium-Ytterbium co-doped Q-switched fiber laser based on nonlinear polarisation rotation technique. Journal of Nonlinear Optical Physics and Materials, 2015, 24, 1550002.	1.8	8
440	Passively Q-switched fiber lasers using a multi-walled carbon nanotube polymer composite based saturable absorber. Optik, 2015, 126, 2950-2954.	2.9	8
441	Fabrication of polymer microfiber through direct drawing and splicing of silica microfiber via vapor spray and flame treatment. Applied Optics, 2015, 54, 3863.	2.1	8
442	Dual-wavelength nano-engineered Thulium-doped fiber laser via bending of singlemode-multimode-singlemode fiber structure. Optical Fiber Technology, 2016, 32, 96-101.	2.7	8
443	Mode-locked generation in thulium-doped fiber linear cavity laser. Optik, 2016, 127, 11119-11123.	2.9	8
444	High-power Q-switched erbium-ytterbium codoped fiber laser using multiwalled carbon nanotubes saturable absorber. Optical Engineering, 2016, 55, 106112.	1.0	8
445	Demonstration of a Periodic Passband Filter Based on Coupled Microfiber Knots. IEEE Photonics Technology Letters, 2016, 28, 1061-1064.	2.5	8
446	Flat-gain wide-band erbium doped fiber amplifier with hybrid gain medium. Optik, 2016, 127, 2481-2484.	2.9	8
447	TEMPERATURE SENSING BY SIDE COUPLING OF LIGHT THROUGH ZINC OXIDE NANORODS ON OPTICAL FIBERS. Sensors and Actuators A: Physical, 2017, 257, 15-19.	4.1	8
448	Passively mode-locked ytterbium-doped fiber laser operation with few layer MoS2 PVA saturable absorber. Optik, 2017, 145, 543-548.	2.9	8
449	Application of MoS ₂ thin film in multi-wavelength and Q-switched EDFL. Journal of Modern Optics, 2017, 64, 457-461.	1.3	8
450	Broadband optical frequency comb generator based on driving N-cascaded modulators by Gaussian-shaped waveform. Optical Fiber Technology, 2018, 42, 75-83.	2.7	8

#	Article	IF	CITATIONS
451	Optical fiber coated Zinc Oxide (ZnO) nanorods decorated with Palladium (Pd) for hydrogen sensing. Optical Materials, 2019, 96, 109291.	3.6	8
452	Q-switched erbium-doped fiber laser using silver nanoparticles deposited onto side-polished D-shaped fiber by electron beam deposition method. Optical Fiber Technology, 2019, 53, 101997.	2.7	8
453	Electron beam deposited silver (Ag) saturable absorber as passive Q-switcher in 1.5- and 2-micron fiber lasers. Optik, 2020, 207, 164455.	2.9	8
454	Ultrafast soliton mode-locked fiber laser at 1560  nm based on Znq ₂ as a saturable absorber. Applied Optics, 2021, 60, 3149.	1.8	8
455	Ultrashort pulse laser at 1564.3Ânm wavelength with E-beam deposited copper nanoparticles saturable absorber. Optics and Laser Technology, 2021, 136, 106791.	4.6	8
456	Nanosecond Q-switched pulse generation using poly(3,4 ethylenedioxythiophene): Poly(4-styrenesulfonate) thin film as saturable absorber. Infrared Physics and Technology, 2021, 116, 103788.	2.9	8
457	Application of black phosphorus for pulse generation in erbium-doped fiber laser. Results in Optics, 2021, 4, 100091.	2.0	8
458	Hygroscopicity Enhancement of Low Temperature Hydrothermally Synthesized Zinc Oxide Nanostructure with Heterocyclic Organic Compound for Humidity Sensitization. Sensors and Actuators B: Chemical, 2021, 345, 130010.	7.8	8
459	Synthesis of silver nanoparticles using chemical reduction techniques for Q-switcher at 1.5µm region. Optik, 2021, 244, 167621.	2.9	8
460	Effect of MAX phase chromium aluminum carbide thin film thickness on Q-switched Erbium-doped fiber lasers. Optical Fiber Technology, 2022, 70, 102853.	2.7	8
461	A Gain-Clamped L-Band Erbium-Doped Fiber Amplifier Using Ring Laser Cavity with a Fiber Bragg Grating. Japanese Journal of Applied Physics, 2002, 41, L836-L838.	1.5	7
462	Self-excited brillouin–erbium fiber laser for DWDM applications. Optics and Laser Technology, 2007, 39, 94-97.	4.6	7
463	Effects of an auxiliary pump on the performance of TDFA. Laser Physics, 2008, 18, 977-982.	1.2	7
464	MULTIWAVELENGTH SOURCE USING A BRILLOUIN FIBER LASER. Journal of Nonlinear Optical Physics and Materials, 2008, 17, 199-203.	1.8	7
465	Optimization of gain flattened C-band EDFA using macro-bending. Laser Physics, 2010, 20, 1433-1437.	1.2	7
466	Low-cost spectral tunable microfibre knot resonator. IET Optoelectronics, 2011, 5, 281.	3.3	7
467	Experimental and theoretical studies on ytterbium sensitized erbium-doped fiber amplifier. Optik, 2011, 122, 1783-1786.	2.9	7
468	Supercontinuum generation in photonic crystal fiber using femtosecond pulses. Laser Physics, 2011, 21, 1215-1218.	1.2	7

#	Article	IF	CITATIONS
469	Fabrication of microfiber loop resonatorâ€based comb filter. Microwave and Optical Technology Letters, 2011, 53, 1119-1121.	1.4	7
470	Fiber optic displacement sensor for microâ€ŧhickness measurement. Sensor Review, 2012, 32, 230-235.	1.8	7
471	Fabrication and Characterization of a 2 × 2 Microfiber Knot Resonator Coupler. Chinese Physics Letters, 2012, 29, 084204.	3.3	7
472	Direct airborne acoustic wave modulation of Fabry–Perot fiber laser (FPFL) over 100ÂkHz of operating bandwidth. Applied Optics, 2012, 51, 2772.	1.8	7
473	Four-Wave-Mixing in Zirconia-Yttria-Aluminum Erbium Codoped Silica Fiber. Journal of the European Optical Society-Rapid Publications, 0, 7, .	1.9	7
474	Multi-wavelength ytterbium doped fiber laser based on longitudinal mode interference. Laser Physics, 2012, 22, 252-255.	1.2	7
475	Q-switched Zr-EDF laser using single-walled CNT/PEO polymer composite as a saturable absorber. Optical Materials, 2013, 35, 347-352.	3.6	7
476	Compact Dual-Wavelength Laser Generation Using Highly Concentrated Erbium-Doped Fiber Loop Attached to Microfiber Coupler. IEEE Journal of Quantum Electronics, 2013, 49, 586-588.	1.9	7
477	Investigation of Bending Sensitivity in Partially Doped Core Fiber for Sensing Applications. IEEE Sensors Journal, 2014, 14, 1295-1303.	4.7	7
478	Q-switched fibre laser using 21cm Bismuth-erbium doped fibre and graphene oxide as saturable absorber. Optics Communications, 2014, 310, 53-57.	2.1	7
479	Q-switched erbium-doped fiber laser using multi-layer graphene based saturable absorber. Journal of Nonlinear Optical Physics and Materials, 2014, 23, 1450009.	1.8	7
480	Dual-wavelength passively Q-switched Erbium Ytterbium codoped fiber laser based on a nonlinear polarization rotation technique. Microwave and Optical Technology Letters, 2015, 57, 530-533.	1.4	7
481	Q-Switched Yb-Doped Fiber Ring Laser with a Saturable Absorber Based on a Graphene Polyvinyl Alcohol Film. Journal of Russian Laser Research, 2015, 36, 389-394.	0.6	7
482	Passive Q-switched and Mode-locked Fiber Lasers Using Carbon-based Saturable Absorbers. , 0, , .		7
483	Highly stable and tunable narrow-spacing dual-wavelength ytterbium-doped fiber using a microfiber Mach–Zehnder interferometer. Optical Engineering, 2016, 55, 026114.	1.0	7
484	Multi-walled carbon nanotubes saturable absorber in Q-switching flashlamp pumped Nd:YAG laser. Optics and Laser Technology, 2016, 79, 193-197.	4.6	7
485	Pure antimony film as saturable absorber for Q-switched erbium-doped fiber laser. Journal of Modern Optics, 2018, 65, 811-817.	1.3	7
486	Optimization of sensing performance factor (<mml:math) (xmlns:n<br="" 0="" 10="" 50="" 72="" etqq0="" overlock="" rgbt="" td="" tf="" tj="">microfiber-coupled ZnO nanorods humidity scheme. Optical Fiber Technology, 2019, 52, 101983.</mml:math)>	nml="http:/ 2.7	//www.w3.org, 7

#	Article	IF	CITATIONS
487	Nanosecond Pulses Generation with Samarium Oxide Film Saturable Absorber*. Chinese Physics Letters, 2019, 36, 074203.	3.3	7
488	Sodium nitrate sensor based on D-shaped fiber structure. Measurement: Journal of the International Measurement Confederation, 2020, 163, 107927.	5.0	7
489	MXene Ti ₃ C ₂ T <i>_x</i> thin film as a saturable absorber for passively mode-locked and Q-switched fibre laser. Journal of Modern Optics, 2021, 68, 984-993.	1.3	7
490	The effects of different parameters and interaction angles of a 532Ânm pulsed Nd: YAG laser on the properties of laser-ablated silver nanoparticles. Optics Communications, 2021, 501, 127366.	2.1	7
491	Lanthanum hexaboride for Q-switching and mode-locking applications. Optics Communications, 2022, 502, 127396.	2.1	7
492	Generation of Q-switched fiber laser at 1.0-, 1.55- and 2.0-µm employing a spent coffee ground based saturable absorber. Optical Fiber Technology, 2021, 61, 102434.	2.7	7
493	Nanosecond pulse generation with a gallium nitride saturable absorber. OSA Continuum, 2019, 2, 134.	1.8	7
494	Q-Switched Ultrafast TDFL Using MWCNTs-SA at 2 Âμm Region. International Journal of Computer and Communication Engineering, 2014, 3, 446-449.	0.2	7
495	Passively mode-locked erbium-doped fiber laser based on a nanodiamond saturable absorber. Applied Optics, 2022, 61, 4047.	1.8	7
496	Q-switched fiber laser in C-band region using metal ceramic-based saturable absorber. Optik, 2022, 264, 169395.	2.9	7
497	Gain-clamping in two-stage L-band EDFA using an unwanted backward ase from second stage. Optics and Laser Technology, 2003, 35, 441-444.	4.6	6
498	An efficient and low noise Gain-Clamped Double-Pass L-Band EDFA. IEICE Electronics Express, 2004, 1, 98-102.	0.8	6
499	Multiwavelength source based on SOA and EDFA in a ring avity resonator. Microwave and Optical Technology Letters, 2009, 51, 110-113.	1.4	6
500	Dual wavelength fibre laser with tunable channel spacing using an SOA and dual AWGs. Journal of Modern Optics, 2009, 56, 1768-1773.	1.3	6
501	Micro-displacement sensor with multimode fused coupler and concave mirror. Laser Physics, 2011, 21, 729-732.	1.2	6
502	Investigation of dispersion characteristic in tapered fiber. Laser Physics, 2011, 21, 945-947.	1.2	6
503	Stable mode-locked fiber laser using 49 cm long bismuth oxide based erbium doped fiber and slow saturable absorber. Laser Physics, 2011, 21, 913-918.	1.2	6
504	Theoretical and experimental studies on liquid refractive index sensor based on bundle fiber. Sensor Review, 2011, 31, 173-177.	1.8	6

#	Article	IF	CITATIONS
505	AQ-switched thulium-doped fiber laser with a graphene thin film based saturable absorber. Laser Physics, 2013, 23, 115102.	1.2	6
506	Evaluation of the tapered PMMA fiber sensor response due to the ionic interaction within electrolytic solutions. Journal of Modern Optics, 2014, 61, 154-160.	1.3	6
507	Qâ€switched thuliumâ€doped fibre laser operating at 1900Ânm using multiâ€layered graphene based saturable absorber. IET Optoelectronics, 2014, 8, 155-160.	3.3	6
508	Gain-shift induced by dopant concentration ratio in a thulium-bismuth doped fiber amplifier. Optics Express, 2014, 22, 7075.	3.4	6
509	Qâ€switched erbium doped fiber laser using singleâ€walled carbon nanotubes embedded in polyethylene oxide film saturable absorber. Microwave and Optical Technology Letters, 2014, 56, 2734-2737.	1.4	6
510	PMMA microfiber coated with ZnO nanostructure for the measurement of relative humidity. IOP Conference Series: Materials Science and Engineering, 2015, 99, 012025.	0.6	6
511	Switchable dual-wavelength CNT-based Q-switched using arrayed waveguide gratings (AWG). Applied Physics B: Lasers and Optics, 2015, 118, 269-274.	2.2	6
512	Application of Fano resonance effects in optical antennas formed by regular clusters of nanospheres. Applied Physics A: Materials Science and Processing, 2015, 118, 139-150.	2.3	6
513	Soliton modeâ€locked erbiumâ€doped fibre laser with mechanically exfoliated molybdenum disulphide saturable absorber. IET Optoelectronics, 2016, 10, 169-173.	3.3	6
514	Generation of an ultra-stable dual-wavelength ytterbium-doped fiber laser using a photonic crystal fiber. Laser Physics, 2016, 26, 025101.	1.2	6
515	Tunable wavelength generation in the 1 <i>µ</i> m region incorporating a 16-channel arrayed waveguide grating (AWG). Laser Physics, 2017, 27, 125101.	1.2	6
516	Uric acid sensing using tapered silica optical fiber coated with zinc oxide nanorods. Microwave and Optical Technology Letters, 2018, 60, 645-650.	1.4	6
517	Passively Q-switched Erbium-Doped Fiber Laser based on Graphene Oxide as Saturable Absorber. Journal of Optical Communications, 2018, 39, 307-310.	4.7	6
518	Singlemode-multimode-singlemode fiber structure as compressive strain sensor on a reinforced concrete beam. Optik, 2018, 154, 705-710.	2.9	6
519	Passively Q-switched erbium-doped fiber laser utilizing lutetium oxide deposited onto D-shaped fiber as saturable absorber. Optik, 2019, 193, 162972.	2.9	6
520	Wide-band flat-gain optical amplifier using Hafnia and zirconia erbium co-doped fibres in double-pass parallel configuration. Journal of Modern Optics, 2019, 66, 1711-1716.	1.3	6
521	Passively Q-switched erbium-doped fiber laser using quantum dots CdSe embedded in polymer film as saturable absorber. Optical and Quantum Electronics, 2019, 51, 1.	3.3	6
522	All fibre Q-switched Thulium-doped fibre laser incorporating Thulium–Holmium co-doped fibre as a saturable absorber. Optics Communications, 2019, 450, 160-165.	2.1	6

#	Article	IF	CITATIONS
523	The effect of 980 nm and 1480 nm pumping on the performance of newly Hafnium Bismuth Erbium-doped fiber amplifier. Journal of Physics: Conference Series, 2019, 1151, 012013.	0.4	6
524	Selfâ€generating Brillouin fiber laser using highly nonlinear hafnium bismuth erbiumâ€doped fiber. Microwave and Optical Technology Letters, 2019, 61, 1651-1655.	1.4	6
525	Titanium dioxide-based picoseconds pulsed fiber laser performances comparison in the 1.5-micron region. Journal of Physics: Conference Series, 2019, 1371, 012023.	0.4	6
526	Theoretical Study on Passively Mode-Locked Fiber Lasers with Saturable Absorber. Fiber and Integrated Optics, 2019, 38, 76-89.	2.5	6
527	Nanosecond pulses generation with rose gold nanoparticles saturable absorber. Indian Journal of Physics, 2020, 94, 1079-1083.	1.8	6
528	Bundled plastic optical fiber based sensor for ECG signal detection. Optik, 2020, 203, 164077.	2.9	6
529	8-Hydroxyquinolino cadmium chloride hydrate for generating nanosecond and picosecond pulses in erbium-doped fiber laser cavity. Optical Fiber Technology, 2021, 61, 102439.	2.7	6
530	Lawsone dye material as potential saturable absorber for Q-switched erbium doped fiber laser. Optical Fiber Technology, 2021, 64, 102537.	2.7	6
531	Development of FBG Humidity Sensor via Controlled Annealing Temperature of Additive Enhanced ZnO Nanostructure Coating. Optical Fiber Technology, 2022, 68, 102802.	2.7	6
532	Nanosecond Q-switched laser with PEDOT: PSS saturable absorber. Applied Optics, 2022, 61, 1292.	1.8	6
533	Qâ€switched neodymiumâ€doped fiber laser with a gold nanoparticleÂsaturable absorber. Microwave and Optical Technology Letters, 2022, 64, 1302-1309.	1.4	6
534	Review: Dark pulse generation in fiber laser system. Optics and Laser Technology, 2022, 151, 108056.	4.6	6
535	Soliton picosecond pulse generation with a spin-coated PEDOT: PSS thin film. Journal of Luminescence, 2022, 247, 118879.	3.1	6
536	Dual-Stage L-Band Erbium-Doped Fiber Amplifier for Gain Enhancement. Japanese Journal of Applied Physics, 2003, 42, L173-L175.	1.5	5
537	A New Gain-Clamped L-Band Erbium-Doped Fiber Amplifier with Highly Efficient Gain. Japanese Journal of Applied Physics, 2003, 42, L930-L931.	1.5	5
538	Gain-clamping techniques in two-stage double-pass L-band EDFA. Pramana - Journal of Physics, 2006, 66, 539-545.	1.8	5
539	S-BAND BRILLOUIN/ERBIUM FIBER LASER FOR DWDM APPLICATION. Journal of Nonlinear Optical Physics and Materials, 2006, 15, 309-313.	1.8	5
540	Linear cavity Brillouin fiber laser using a fiber Bragg grating. Microwave and Optical Technology Letters, 2008, 50, 265-266.	1.4	5

#	Article	IF	CITATIONS
541	Effect of tilting angles on the performance of reflective and transmitting types of fiber optic-based displacement sensors. Laser Physics, 2010, 20, 824-829.	1.2	5
542	Investigation on stimulated Brillouin scattering characteristics in a highly doped Bismuth-based Erbium-doped fiber. Laser Physics, 2010, 20, 1973-1977.	1.2	5
543	Broadband ASE source using bismuth-based erbium-doped fibers in double-pass set-up. Microwave and Optical Technology Letters, 2010, 52, 1636-1638.	1.4	5
544	BRILLOUIN–RAMAN MULTI-WAVELENGTH LASER COMB GENERATION BASED ON Bi-EDF BY USING DUAL-WAVELENGTH IN DISPERSION COMPENSATING FIBER. Journal of Nonlinear Optical Physics and Materials, 2010, 19, 123-130.	1.8	5
545	Wavelength conversion based on FWM in a HNLF by using a tunable dual-wavelength erbium doped fibre laser source. Journal of Modern Optics, 2011, 58, 566-572.	1.3	5
546	Stable power multi-wavelength fibre laser based on four-wave mixing in a short length of highly non-linear fibre. Journal of Optics (United Kingdom), 2011, 13, 075401.	2.2	5
547	Highly efficient short length Bismuth-based erbium-doped fiber amplifier. Laser Physics, 2011, 21, 1793-1796.	1.2	5
548	Wavelength conversion based on four-wave mixing in a highly nonlinear fiber in ring configuration. Laser Physics Letters, 2011, 8, 742-746.	1.4	5
549	Investigation on stimulated Brillouin scattering effect in Photonic crystal fiber. Microwave and Optical Technology Letters, 2011, 53, 1450-1453.	1.4	5
550	Fiber optic chemical sensor using fiber coupler probe based on intensity modulation for alcohol detection. Microwave and Optical Technology Letters, 2011, 53, 1935-1938.	1.4	5
551	1880-nm Broadband ASE Generation With Bismuth–Thulium Codoped Fiber. IEEE Photonics Journal, 2012, 4, 2176-2181.	2.0	5
552	Four-wave mixing in zirconia-erbium doped fiber – a comparison between ring and linear cavities. Laser Physics Letters, 2012, 9, 819-825.	1.4	5
553	Thermal response of chalcogenide microsphere resonators. Quantum Electronics, 2012, 42, 462-464.	1.0	5
554	Comparison between Analytical Solution and Experimental Setup of a Short Long Ytterbium Doped Fiber Laser. Optics and Photonics Journal, 2012, 02, 65-72.	0.4	5
555	Thermally tunable microfiber knot resonator based erbium-doped fiber laser. Optics Communications, 2012, 285, 4684-4687.	2.1	5
556	Passively modeâ€locked soliton fiber laser using a combination of saturable absorber and nonlinear polarization rotation technique. Microwave and Optical Technology Letters, 2012, 54, 1430-1432.	1.4	5
557	Transmission characteristic of multi-turn microfiber coil resonator. Optics and Laser Technology, 2012, 44, 1791-1795.	4.6	5
558	Multi-wavelength Brillouin fiber laser generation using dual-pass approach. Laser Physics, 2012, 22, 584-587.	1.2	5

#	Article	IF	CITATIONS
559	Detection of stain formation on teeth by oral antiseptic solution using fiber optic displacement sensor. Optics and Laser Technology, 2013, 45, 336-341.	4.6	5
560	Temperature-Insensitive Bend Sensor Using Entirely Centered Erbium Doping in the Fiber Core. Sensors, 2013, 13, 9536-9546.	3.8	5
561	Q-Switching and Mode-Locking in Highly Doped Zr\$_{2}\$O\$_{3}\$–Al\$_{2}\$ O\$_{3}\$–Er \$_{2}\$O\$_{3}\$-Doped Fiber Lasers Using Graphene as a Saturable Absorber. IEEE Journal of Selected Topics in Quantum Electronics, 2014, 20, 9-16.	2.9	5
562	All-fiber dual wavelength passive Q-switched fiber laser using a dispersion-decreasing taper fiber in a nonlinear loop mirror. Optics Express, 2014, 22, 22794.	3.4	5
563	Multi-wavelength fiber laser generation by using optical wavelength conversion. Laser Physics, 2014, 24, 065105.	1.2	5
564	Flat-gain wide-band erbium doped fiber amplifier by combining two difference doped fibers. Journal of the European Optical Society-Rapid Publications, 0, 10, .	1.9	5
565	Multimode interference in single modeâ€multimodeâ€single mode fiber structure for steel beam compressive strain measurement. Microwave and Optical Technology Letters, 2018, 60, 1971-1975.	1.4	5
566	MWCNTs coated silica microfiber sensor for detecting Mg2+ in de-ionized water. Optik, 2018, 171, 65-70.	2.9	5
567	Q-switched fiber laser operating at 1 μm region with electron beam deposited titanium nanoparticles. Optics and Laser Technology, 2019, 120, 105702.	4.6	5
568	A study on relative humidity sensors using PVA and PMMA coating. Journal of Physics: Conference Series, 2019, 1371, 012027.	0.4	5
569	Passively Q-switched fibre laser utilizing erbium-doped fibre saturable absorber for operation in C-band region. Journal of Modern Optics, 2019, 66, 235-239.	1.3	5
570	Performance comparison of high temperature sensor based on nonâ€adiabatic silica microfiber and single modeâ€multimodeâ€single mode fiber structure. Microwave and Optical Technology Letters, 2019, 61, 431-435.	1.4	5
571	Investigation of the Brillouin effect in highly nonlinear hafnium bismuth erbium doped fiber. Microwave and Optical Technology Letters, 2019, 61, 173-177.	1.4	5
572	Newly developed chromium-doped fiber as a saturable absorber at 1.55- and 2.0-µm regions for Q-switching pulses generation. Optical Fiber Technology, 2019, 48, 144-150.	2.7	5
573	Low-profile folded dipole UHF RFID tag antenna with outer strip lines for metal mounting application. Turkish Journal of Electrical Engineering and Computer Sciences, 2020, 28, 2643-2656.	1.4	5
574	Inducing Q-switching operation at 1-micron all-fiber laser via lutetium oxide film saturable absorber. Optik, 2020, 219, 165267.	2.9	5
575	Optical and Photoacoustic Properties of Laser-Ablated Silver Nanoparticles in a Carbon Dots Solution. Molecules, 2020, 25, 5798.	3.8	5
576	Bismuthâ€doped fiber as <i>Q</i> â€switcher in hafnium bismuth erbium coâ€doped fiber laser. Microwave and Optical Technology Letters, 2020, 62, 3634-3639.	1.4	5

#	Article	IF	CITATIONS
577	Zinc phthalocyanine thin film as saturable absorber for Q-switched pulse generation. Optical Fiber Technology, 2020, 57, 102235.	2.7	5
578	MEH-PPV organic material as saturable absorber for Q-switching and mode-locking applications. Journal of Modern Optics, 2020, 67, 746-753.	1.3	5
579	Thulium oxide film as a passive saturable absorber for pulsed fiber laser generation. Optical Fiber Technology, 2020, 58, 102249.	2.7	5
580	Detection of seismograph signal using fiber bundle sensor. Optik, 2020, 208, 164554.	2.9	5
581	Bismuthâ€doped fiber Qâ€switcher in erbiumâ€doped fiber laser cavity. Microwave and Optical Technology Letters, 2021, 63, 2214-2218.	1.4	5
582	Thermally stable and fast responsive mesoporous cresol red functionalized silica and titania nanomatrices: fiber optic pH sensors. Journal of Sol-Gel Science and Technology, 2021, 99, 497-511.	2.4	5
583	Absorption, fluorescence and sensing quality of Rose Bengal dye-encapsulated cinnamon nanoparticles. Sensors and Actuators A: Physical, 2021, 332, 113055.	4.1	5
584	Dual-wavelength passively Q-switched Erbium-doped fiber laser with MWCNTs slurry as saturable absorber. Photonics Letters of Poland, 2016, 8, 98.	0.4	5
585	Graphene/PVA coated D-shaped fiber for sodium nitrate sensing. Sensors and Actuators A: Physical, 2021, 332, 113163.	4.1	5
586	Generation of Q-switched and mode-locked pulses using neodymium oxide as saturable absorber. Results in Optics, 2020, 1, 100032.	2.0	5
587	Ultrashort pulse generation in All-fiber Erbium-doped fiber cavity with thulium doped fiber saturable absorber. Optics and Laser Technology, 2022, 149, 107888.	4.6	5
588	Yttrium Oxide (Y2O3) as a Pulse Initiator in a Mode-Locking Erbium-Doped Fiber Laser. Photonics, 2022, 9, 486.	2.0	5
589	Gain-clamped two-stage L-band EDFA with a FBG laser in second stage. Optics and Laser Technology, 2003, 35, 645-647.	4.6	4
590	An Enhanced Bismuth-Based Brillouin/Erbium Fiber Laser with Linear Cavity Configuration. Fiber and Integrated Optics, 2007, 27, 35-40.	2.5	4
591	SOA based fiber ring laser with Fiber Bragg Grating. Microwave and Optical Technology Letters, 2008, 50, 3101-3103.	1.4	4
592	Gain improvement in a dual-stage S-band EDFA by filtration of forward C-band ASE. Journal of Modern Optics, 2008, 55, 3035-3040.	1.3	4
593	CONTROLLABLE WAVELENGTH CHANNELS FOR MULTIWAVELENGTH BRILLOUIN BISMUTH/ERBIUM BASED FIBER LASER. Progress in Electromagnetics Research Letters, 2009, 9, 9-18.	0.7	4
594	THE COMPARISON NONLINEARITY BEHAVIORS OF PHOTONIC CRYSTAL FIBER BY TWO REDUCED LENGTHS OF BI-EDF IN RING CAVITY. Journal of Nonlinear Optical Physics and Materials, 2009, 18, 521-527.	1.8	4

#	Article	IF	CITATIONS
595	A theoretical study of double-pass thulium-doped fiber amplifiers. Optik, 2010, 121, 1257-1262.	2.9	4
596	TEMPERATURE INSENSITIVE BROAD AND FLAT GAIN C-BAND EDFA BASED ON MACRO-BENDING. Progress in Electromagnetics Research C, 2010, 15, 37-48.	0.9	4
597	Efficient diode pumped ytterbium-doped fibre laser. Electronics Letters, 2010, 46, 68.	1.0	4
598	Effects of Pumping Scheme and Double-Propagation on the Performance of ASE Source using Dual-Stage Bismuth-Based Erbium-Doped Fiber. Journal of Electromagnetic Waves and Applications, 2010, 24, 373-381.	1.6	4
599	Investigation of the effects of SOA locations in the linear cavity of an O-band Brillouin SOA fiber laser. Journal of Modern Optics, 2011, 58, 580-586.	1.3	4
600	High output power, narrow linewidth Brillouin fibre laser master-oscillator/power-amplifier source. IET Optoelectronics, 2011, 5, 181-183.	3.3	4
601	Operation of brillouin fiber laser in the O-band region as compared to that in the C-band region. Laser Physics, 2011, 21, 210-214.	1.2	4
602	Double spacing multi-wavelength L-band Brillouin erbium fiber laser with Raman pump. Journal of Modern Optics, 2012, 59, 1690-1694.	1.3	4
603	Wideband and flat-gain amplifier based on high concentration erbium-doped fibres in parallel double-pass configuration. Quantum Electronics, 2012, 42, 241-243.	1.0	4
604	Feasibility of fiber optic displacement sensor scanning system for imaging of dental cavity. Journal of Biomedical Optics, 2012, 17, 071308.	2.6	4
605	Fano resonance on plasmonic nanostructures. , 2012, , .		4
606	S-band gain and noise figure improvements in thulium-doped fiber amplifier by using macro-bending approach. Applied Physics B: Lasers and Optics, 2012, 108, 807-813.	2.2	4
607	Theoretical and experimental studies on coupler based fiber optic displacement sensor with concave mirror. Optik, 2012, 123, 2105-2108.	2.9	4
608	Passively Q-Switched 11-Channel Stable Brillouin Erbium-Doped Fiber Laser With Graphene as the Saturable Absorber. IEEE Photonics Journal, 2012, 4, 2050-2056.	2.0	4
609	Wideband and compact erbiumâ€doped fiber amplifier using parallel doubleâ€pass configuration. Microwave and Optical Technology Letters, 2012, 54, 629-631.	1.4	4
610	Synchronous tunable wavelength spacing dual-wavelength SOA fiber ring laser using Fiber Bragg grating pair in a hybrid tuning package. Optics Communications, 2012, 285, 1326-1330.	2.1	4
611	Effect of doped fiber length on the stretch pulses of a mode-locked erbium-doped fiber laser. Laser Physics, 2012, 22, 1240-1243.	1.2	4
612	Effect of loop diameter on the performance of MKRâ€based dualâ€wavelength erbiumâ€doped fiber laser. Microwave and Optical Technology Letters, 2013, 55, 236-238.	1.4	4

#	Article	IF	CITATIONS
613	Nanosecond Pulse Generation Using the Stimulated Brillouin Scattering Effect in a Photonic Crystal Fiber. Chinese Physics Letters, 2013, 30, 114204.	3.3	4
614	Tapered Fiber Coated with Hydroxyethyl Cellulose/Polyvinylidene Fluoride Composite for Relative Humidity Sensor. Advances in Materials Science and Engineering, 2013, 2013, 1-4.	1.8	4
615	Q-switched multi-wavelength Brillouin erbium fiber laser. Journal of Nonlinear Optical Physics and Materials, 2014, 23, 1450010.	1.8	4
616	Tunable single Stokes extraction from 20  GHz Brillouin fiber laser using ultranarrow bandwidth optical filter. Applied Optics, 2014, 53, 6944.	1.8	4
617	Qâ€switching and modeâ€locking pulse generation with graphene oxide paperâ€based saturable absorber. Journal of Engineering, 2015, 2015, 208-214.	1.1	4
618	DETECTION OF DIFFERENT CONCENTRATIONS OF URIC ACID USING TAPERED SILICA OPTICAL SENSOR COATED WITH ZINC OXIDE (ZNO). Jurnal Teknologi (Sciences and Engineering), 2015, 74, .	0.4	4
619	Qâ€switched thulium–ytterbium coâ€doped fibre laser using newly developed octagonal shaped inner cladding doubleâ€clad active fibre and multiâ€walled carbon nanotubes passive saturable absorber. IET Optoelectronics, 2015, 9, 131-135.	3.3	4
620	Dual Output Approach in Dye Concentrations Determination Using Non-Adiabatic Tapered Fiber. IEEE Sensors Journal, 2015, 15, 3903-3908.	4.7	4
621	Performance of passively Qâ€switched ring erbiumâ€doped fiber laser using a multiwalled carbon nanotubes polyethylene oxide (PEO) polymer compositeâ€based saturable absorber. Microwave and Optical Technology Letters, 2015, 57, 1897-1901.	1.4	4
622	Qâ€switched Brillouin fibre laser with multiâ€wall carbon nanotube saturable absorber. IET Optoelectronics, 2015, 9, 96-100.	3.3	4
623	Q-switched 2µm thulium bismuth co-doped fiber laser with multi-walled carbon nanotubes saturable absorber. Optics and Laser Technology, 2016, 83, 89-93.	4.6	4
624	Q-switched thulium-doped fiber laser operating at 1940Ânm region using a pencil-core as saturable absorber. Journal of Modern Optics, 2016, 63, 783-787.	1.3	4
625	Passively Q-switched Ytterbium doped fiber laser with mechanically exfoliated MoS2 saturable absorber. Indian Journal of Physics, 2017, 91, 575-580.	1.8	4
626	Water wave gauge based on singlemode-multimode-singlemode fiber structure. Optik, 2017, 144, 232-239.	2.9	4
627	Effect of Polymerization Temperatures on Polyaniline Coated Fiber Bragg Grating Sensor for Chloroform Detection. Macromolecular Symposia, 2018, 382, 1800088.	0.7	4
628	Effect of tapering diameters with microbottle resonator for formaldehyde (CH2O) liquid sensing. Sensing and Bio-Sensing Research, 2019, 25, 100292.	4.2	4
629	Generation of bound state of solitons pulses with graphene in Erbium-doped fiber laser cavity. Journal of Physics: Conference Series, 2019, 1151, 012017.	0.4	4
630	Q-switched erbium-doped fiber lasers based on copper nanoparticles saturable absorber. Journal of Physics: Conference Series, 2019, 1371, 012028.	0.4	4

#	Article	IF	CITATIONS
631	Passively Q-switched fiber laser tunable by Sagnac interferometer operation. Optik, 2019, 179, 1-7.	2.9	4
632	Qâ€ s witching pulses generation with samarium oxide film saturable absorber. Microwave and Optical Technology Letters, 2020, 62, 1049-1055.	1.4	4
633	Optical fiber coated with zinc oxide nanorods toward light side coupling for sensing application. , 2020, , 293-304.		4
634	Generation of Q-switched Erbium-Doped Fiber Laser Using Titanium Dioxide Film Based Saturable Absorber. IOP Conference Series: Materials Science and Engineering, 2020, 854, 012018.	0.6	4
635	Microbottle-Resonator Ethanol Liquid Sensor. IOP Conference Series: Materials Science and Engineering, 2020, 854, 012075.	0.6	4
636	Sc ₂ O ₃ PVA Film for Switching and Mode-Locking Application in Erbium-Doped Fiber Laser Cavity. Fiber and Integrated Optics, 2020, 39, 137-148.	2.5	4
637	Copper nanoparticles-chitosan based saturable absorber in passively Q-switched erbium doped fiber laser. AIP Conference Proceedings, 2020, , .	0.4	4
638	Optically functionalized hierarchical hematite assembled silica-titania nanocomposites for hydrocarbon detection: Fiber optic chemical sensor. Microporous and Mesoporous Materials, 2021, 326, 111398.	4.4	4
639	Polyvinyl alcohol coating microbottle resonator on whispering gallery modes for ethanol liquid sensor. Optics and Laser Technology, 2021, 143, 107379.	4.6	4
640	Q-switched fiber laser with tunable wavelength operation utilizing a nonlinear saturable absorption of vanadium pentoxide. Indian Journal of Physics, 2022, 96, 281-287.	1.8	4
641	Femtosecond modeâ€locked erbiumâ€doped fibre laser with Alq 3 saturable absorber. IET Optoelectronics, 2020, 14, 234-241.	3.3	4
642	Q-switched ytterbium-doped fiber laser by using FIrpic as a saturable absorber. OSA Continuum, 2019, 2, 2145.	1.8	4
643	Bismuth (III) Telluride (Bi2Te3) topological insulator embed in PVA as passive Q-switcher at 2 micron region. Photonics Letters of Poland, 2016, 8, 101.	0.4	4
644	Evanescent field interaction of 1550Ânm pulsed laser with silver nanomaterial coated D-shape fiber. Infrared Physics and Technology, 2021, 119, 103920.	2.9	4
645	Enhanced fiber mounting and etching technique for optimized optical power transmission at critical cladding thickness for fiber-sensing application. Laser Physics, 2021, 31, 126201.	1.2	4
646	Optical Microfiber Sensor : A Review. Journal of Physics: Conference Series, 2021, 2075, 012021.	0.4	4
647	Gain clamped L-band EDFA using a fiber Bragg grating in two stage configuration. Microwave and Optical Technology Letters, 2003, 37, 265-266.	1.4	3
648	Effect of injection of C-band ASE on L-band erbium-doped fiber amplifier. JETP Letters, 2003, 77, 461-463.	1.4	3

Sulaiman W Harun

#	Article	IF	CITATIONS
649	Gain Clamped Two-Stage Double-Pass L-Band EDFA with a Single Fibre Bragg Grating. Chinese Physics Letters, 2004, 21, 1954-1957.	3.3	3
650	Gain control in double-pass L-band EDFA using a ring resonator and two-stage configuration. Optik, 2004, 115, 525-527.	2.9	3
651	Efficient and low-noise gain-flattened double-pass L-band erbium-doped fiber amplifier. Microwave and Optical Technology Letters, 2004, 40, 112-114.	1.4	3
652	A Partial Double-Pass S-Band Erbium-Doped Fibre Amplifier. Chinese Physics Letters, 2005, 22, 3080-3082.	3.3	3
653	An efficient S-band brillouin erbium fiber laser with additional EDFA. Optics and Laser Technology, 2007, 39, 616-618.	4.6	3
654	Stopping and storing light pulses within a fiber optic ring resonator. Chinese Optics Letters, 2009, 7, 778-780.	2.9	3
655	Multiple Brillouin Stokes generation with bismuthâ€based erbiumâ€doped fiber. Microwave and Optical Technology Letters, 2010, 52, 1416-1418.	1.4	3
656	Temperature sensor based on fluorescence measurement of Cerium Ytterbium doped fiber. Optics and Spectroscopy (English Translation of Optika I Spektroskopiya), 2011, 111, 312-314.	0.6	3
657	High gain S-band semiconductors optical amplifier with double-pass configuration. Laser Physics, 2011, 21, 1208-1211.	1.2	3
658	Four-wave mixing in dual wavelength fiber laser utilizing SOA for wavelength conversion. Optik, 2011, 122, 754-757.	2.9	3
659	Effect of Q-switched pulses exposure on morphology, hydroxyapatite composition, and microhardness properties of human enamel. Journal of Laser Applications, 2011, 23, 032006.	1.7	3
660	Fiber optical based parametric amplifier in a highly nonlinear fiber (HNLF) by using a ring configuration. Journal of Modern Optics, 2011, 58, 1065-1069.	1.3	3
661	Fiber optic displacement sensor using fiber coupler probe and real objects. Sensor Review, 2012, 32, 212-216.	1.8	3
662	OPTICAL AMPLIFIER WITH FLAT-GAIN AND WIDEBAND OPERATION UTILIZING HIGHLY CONCENTRATED ERBIUM-DOPED FIBERS. Journal of Nonlinear Optical Physics and Materials, 2012, 21, 1250005.	1.8	3
663	Erbium-Doped Fiber Laser With a Microfiber Coupled to Silica Microsphere. IEEE Photonics Journal, 2012, 4, 1065-1070.	2.0	3
664	Quantitative analysis of energy transfer processes in Thulium–Bismuth germanate co-doped fiber amplifier. Optical Materials, 2012, 35, 231-239.	3.6	3
665	Compact and wide-band bismuth-based erbium-doped fibre amplifier based on two-stage and double-pass approaches. IET Optoelectronics, 2012, 6, 127.	3.3	3
666	Broad spectral sliced multiwavelength source with a mode locked fiber laser. Laser Physics, 2012, 22, 212-215.	1.2	3

#	Article	IF	CITATIONS
667	Generation of high power pulse of Biâ€EDF and octave spanning supercontinuum using highly nonlinear fiber. Microwave and Optical Technology Letters, 2012, 54, 983-987.	1.4	3
668	Wide-band fanned-out supercontinuum source covering O-, E-, S-, C-, L- and U-bands. Optics and Laser Technology, 2012, 44, 2168-2174.	4.6	3
669	Stable zirconia-erbium doped multiwavelength fiber laser by precise control of polarization states. Laser Physics, 2012, 22, 982-985.	1.2	3
670	Extraction of a single Stokes line from a Brillouin fibre laser using a silicon oxynitride microring filter. Laser Physics, 2013, 23, 095102.	1.2	3
671	Allâ€Fiber Dualâ€Wavelength Thulium–Bismuth Codoped Fiber Laser. Microwave and Optical Technology Letters, 2013, 55, 2324-2326.	1.4	3
672	Q-switched and soliton pulses generation based on carbon nanotubes saturable absorber. , 2013, , .		3
673	A Tm-Bi Co-Doped Fiber Laser with Dual Pumping Operation. Chinese Physics Letters, 2013, 30, 034204.	3.3	3
674	Effects of Yb/Tm Concentration and Pump Wavelength on the Performance of Ytterbium-Sensitized Thulium-Doped Fiber Laser. IEEE Journal of Quantum Electronics, 2013, 49, 95-99.	1.9	3
675	Nanosecond pulse fibre laser based on nonlinear polarisation rotation effect. Electronics Letters, 2013, 49, 1240-1241.	1.0	3
676	MULTIWAVELENGTH BRILLOUIN-ERBIUM FIBER LASER GENERATION WITH DOUBLE-BRILLOUIN-FREQUENCY SPACING IN A RING CAVITY. Journal of Nonlinear Optical Physics and Materials, 2013, 22, 1350021.	1.8	3
677	Classification of reflected signals from cavitated tooth surfaces using an artificial intelligence technique incorporating a fiber optic displacement sensor. Journal of Biomedical Optics, 2014, 19, 057009.	2.6	3
678	Investigation of spontaneous Brillouin scattering generation based on non-adiabatic microfibres. Laser Physics Letters, 2014, 11, 125105.	1.4	3
679	Single-longitudinal-mode operation in tunable novel zirconia–yttria–alumina–erbium-doped fiber laser. Laser Physics, 2014, 24, 085106.	1.2	3
680	A passively harmonically modeâ€locked soliton erbiumâ€doped fiber laser with low pumping threshold using a singleâ€walled carbon nanotubes. Microwave and Optical Technology Letters, 2015, 57, 799-803.	1.4	3
681	Modeling the Concentric Fiber Optic Bundle Displacement Sensor Using a Quasi-Gaussian Beam Approach. IEEE Sensors Journal, 2015, 15, 4777-4781.	4.7	3
682	Performance enhancement of pre-spectrum slicing technique for wavelength conversion. Optics Communications, 2015, 350, 154-159.	2.1	3
683	Effective use of an EDFA and Raman pump residual powers via a Bi-EDF in L-band multi-wavelength fiber laser generation. Laser Physics, 2015, 25, 015104.	1.2	3
684	Dynamic characteristics of a multi-wavelength Brillouin–Raman fiber laser assisted by multiple four-wave mixing processes in a ring cavity. Optics and Laser Technology, 2015, 66, 63-67.	4.6	3

#	Article	IF	CITATIONS
685	Optical based relative humidity sensor using tapered optical fiber coated with graphene oxide. , 2016, , .		3
686	Multi-wavelength mode-locked erbium-doped fiber laser with photonic crystal fiber in figure-of-eight cavity. Optik, 2016, 127, 5894-5898.	2.9	3
687	Dye Concentrations Measurement Using Mach–Zehner Interferometer Sensor and Modeled by ANFIS. IEEE Sensors Journal, 2016, 16, 8044-8050.	4.7	3
688	Generation of stable and narrow spacing dual-wavelength ytterbium-doped fiber laser using a photonic crystal fiber. Journal of Modern Optics, 2016, 63, 968-973.	1.3	3
689	Dye concentration determination with cross-sensitivity compensation. Sensors and Actuators B: Chemical, 2016, 226, 450-456.	7.8	3
690	A simple load sensor based on a bent single-mode-multimode-single-mode fiber structure. Sensors and Actuators A: Physical, 2016, 242, 106-110.	4.1	3
691	Multiwavelength Brillouin fibre laser in two-mode fiber. Journal of Modern Optics, 2017, 64, 1744-1750.	1.3	3
692	Growth of well-arrayed ZnO nanorods on single-mode silica fiber and evaluation of its light scattering. Microwave and Optical Technology Letters, 2017, 59, 2196-2201.	1.4	3
693	Application of Fiber Bragg Grating Sensor coated with Polyaniline as an optical Sensor for chloroform detection. Polymers and Polymer Composites, 2017, 25, 555-562.	1.9	3
694	Bismuth (III) Telluride (Bi2Te3) Based Topological Insulator Embedded in PVA as Passive Saturable Absorber in Erbium-Doped Fiber Laser. IOP Conference Series: Materials Science and Engineering, 2017, 210, 012032.	0.6	3
695	The generation of Q-switched erbium-doped fiber laser using black phosphorus saturable absorber with 8% modulation depth. IOP Conference Series: Materials Science and Engineering, 2017, 210, 012043.	0.6	3
696	Holmium based nanoseconds pulsed fibre laser generation in the 2-micron region. Optik, 2019, 195, 163157.	2.9	3
697	An efficient <i>L</i> -band Zirconia Yttria Aluminum Erbium co-doped fiber amplifier with 1480nm pumping. Journal of Nonlinear Optical Physics and Materials, 2019, 28, 1950018.	1.8	3
698	Ytterbium doped fiber saturable absorber for a stable passively Q-switched fiber laser in the 1-micron region. Journal of Physics: Conference Series, 2019, 1151, 012008.	0.4	3
699	Side-Polished Optical Fiber Structure for Sodium Nitrate Sensor. IEEE Sensors Journal, 2020, 20, 5929-5934.	4.7	3
700	C-band tunable Q-switched fiber laser based on Alq3 as a saturable absorber. Results in Optics, 2021, 2, 100036.	2.0	3
701	Performance analysis of WDM-SDM system with employing Phase-Conjugated twin waves technique. Materials Today: Proceedings, 2021, 42, 2490-2496.	1.8	3
702	Characterization of hysteresis free, low-temperature hydrothermally synthesized zinc oxide for enhanced humidity sensing. Sensors International, 2021, 2, 100106.	8.4	3

#	Article	IF	CITATIONS
703	Passively Q-switched erbium-doped fiber laser with graphene oxide film as saturable absorber. Journal of Physics: Conference Series, 2021, 1869, 012158.	0.4	3
704	Gold nanoparticles film for Q-switched pulse generation in thulium doped fiber laser cavity. Optoelectronics Letters, 2021, 17, 449-453.	0.8	3
705	Qâ€switched thuliumâ€doped fibre laser operating at 1900Ânm using multiâ€walled carbon nanotubes saturable absorber. Journal of Engineering, 2014, 2014, 297-301.	1.1	3
706	Multiwavelength Q-switched pulse operation with gold nanoparticles as saturable absorber. Optical Engineering, 2019, 58, 1.	1.0	3
707	Q-switched ytterbium-doped fiber laser based on evanescent field interaction with lutetium oxide. Applied Optics, 2019, 58, 9670.	1.8	3
708	Passively Q-switched erbium-doped fiber laser utilizing tungsten oxide as a saturable absorber. Applied Optics, 2019, 58, 9768.	1.8	3
709	Mode-locked Thulium Ytterbium co-Doped Fiber Laser with Graphene Saturable Absorber. Photonics Letters of Poland, 2016, 8, 104.	0.4	3
710	Graphene Oxide Film as Passive Q-switcher in Erbium-doped Fiber Laser Cavity. Photonics Letters of Poland, 2017, 9, 100.	0.4	3
711	Poly(3,4-ethylenedioxythiophene): Poly(styrenesulfonate) spin-coated onto polyvinyl alcohol film as saturable absorber for generating Q-switched laser at 1.5µm region. Optical Fiber Technology, 2022, 68, 102763.	2.7	3
712	A tunable optical frequency comb source using cascaded frequency modulator and Mach–Zehnder modulators. Journal of Optical Communications, 2020, .	4.7	3
713	Mode-locked ytterbium-doped fiber laser with zinc phthalocyanine thin film saturable absorber. Frontiers of Optoelectronics, 2022, 15, .	3.7	3
714	Passively mode-locked laser using HfSe2 as saturable absorber at 1.5Âμm and 2.0Âμm. Optics and Laser Technology, 2022, 155, 108397.	4.6	3
715	Gain and Noise Figure Improvements in Double Pass L-band EDFA using a Band-pass Filter. Journal of Optical Communications, 2002, 23, .	4.7	2
716	Double pass L-band EDFA incorporating band pass filter. , 0, , .		2
717	High gain L-band erbium-doped fiber amplifier with two-stage double-pass configuration. Pramana - Journal of Physics, 2003, 61, 93-97.	1.8	2
718	Gain-Clamped L-Band Erbium-Doped Fiber Amplifier with Co- and Counter-Propagating Lasers. Japanese Journal of Applied Physics, 2003, 42, L1262-L1264.	1.5	2
719	Tunable and Low Noise Gain-Clamped Double-Pass L-Band Erbium-Doped Fiber Amplifier. Japanese Journal of Applied Physics, 2004, 43, L1075-L1077.	1.5	2
720	Gain-Clamped Double-Pass L-Band Erbium-Doped Fiber Amplifier Using A Ring Laser and Fiber Bragg Grating. Japanese Journal of Applied Physics, 2004, 43, L924-L926.	1.5	2

Sulaiman W Harun

#	Article	IF	CITATIONS
721	Partial gain-clamping in two-stage double-pass L-band EDFA using a ring resonator. , 2004, , .		2
722	ASE Spectral Slice Gain-Clamping of EDFA. IEEE Photonics Technology Letters, 2004, 16, 2604-2606.	2.5	2
723	Gain control in S-band erbium-doped fiber amplifier using a fiber bragg grating. IEICE Electronics Express, 2005, 2, 186-191.	0.8	2
724	An enhanced S-band brillouin/erbium fiber laser with an additional EDFA in sub-loop. IEICE Electronics Express, 2005, 2, 321-326.	0.8	2
725	Two-stage S-band erbium-doped fiber amplifier using a depressed-cladding fiber. Microwave and Optical Technology Letters, 2005, 46, 92-94.	1.4	2
726	Highly saturated EDFA for gain clamping operation. Microwave and Optical Technology Letters, 2007, 49, 1815-1816.	1.4	2
727	Brillouin Erbium Ytterbium Fiber Laser. , 2008, , .		2
728	SOA-based multi-wavelength source. Journal of Modern Optics, 2008, 55, 2179-2185.	1.3	2
729	COMPACT AND EFFICIENT Er – Yb -DOPED FIBER AMPLIFIER. Journal of Nonlinear Optical Physics and Materials, 2008, 17, 193-198.	1.8	2
730	Shorter Wavelength Gain Shift In EDFA Using A Macro-Bending Approach. , 2008, , .		2
731	Optimization of fiber length and bending Diameter in depressed cladding Erbium-doped Fiber Amplifier. , 2009, , .		2
732	Effect of gain medium on the performance of Brillouin fiber laser. Microwave and Optical Technology Letters, 2010, 52, 2158-2160.	1.4	2
733	O -BAND MULTI-WAVELENGTH FIBER LASER. Journal of Nonlinear Optical Physics and Materials, 2010, 19, 229-236.	1.8	2
734	O-band to C-band wavelength converter by using four-wave mixing effect in 1310 nm SOA. Journal of Modern Optics, 2010, 57, 2147-2153.	1.3	2
735	An Efficient Photonic Crystal Fiber-Based Brillouin Erbium Fiber Laser Using a Fiber Bragg Grating for Multi-Wavelength Generation. Fiber and Integrated Optics, 2011, 30, 259-264.	2.5	2
736	Fabrication and characterization of optical microfiber structures. , 2011, , .		2
737	Dual-wavelength laser generation using highly concentrated erbium-doped fibre coupling with microfibre knot resonator. Electronics Letters, 2012, 48, 278.	1.0	2
738	Broadband amplifier and high performance tunable laser with an extinction ratio of higher than 60 dB using bismuth oxide-based erbium-doped fiber. Journal of Modern Optics, 2012, 59, 1106-1112.	1.3	2

#	Article	IF	CITATIONS
739	MICROFIBER STRUCTURES FOR SENSOR APPLICATIONS. Journal of Nonlinear Optical Physics and Materials, 2012, 21, 1250003.	1.8	2
740	Supercontinuum generation using a passive mode-locked stretched-pulse bismuth-based erbium-doped fiber laser. Optics and Laser Technology, 2012, 44, 741-743.	4.6	2
741	Generation of efficient 20 GHz optical combs in a Brillouin-erbium fiber laser. Laser Physics, 2013, 23, 015103.	1.2	2
742	Relative humidity measurement using tapered plastic fiber coated with HEC/PVDF. , 2013, , .		2
743	Investigation of Q-Switching Characteristics in Single- and Double-Spacing Multi-Wavelength Brillouin Erbium Fiber Laser. IEEE Photonics Journal, 2013, 5, 1400206-1400206.	2.0	2
744	Quantification of Mesenchymal Stem Cell Growth Rates through Secretory and Excretory Biomolecules in Conditioned Media via Fresnel Reflection. Sensors, 2013, 13, 13276-13288.	3.8	2
745	Tunable S-band output based on Raman shift in dispersion shifted fiber. Journal of Modern Optics, 2013, 60, 737-740.	1.3	2
746	S-band SLM distributed Bragg reflector fiber laser. Laser Physics, 2014, 24, 065109.	1.2	2
747	A Mode-Locked Soliton Erbium-Doped Fiber Laser with a Single-Walled Carbon Nanotube Poly-Ethylene Oxide Film Saturable Absorber. Chinese Physics Letters, 2014, 31, 094202.	3.3	2
748	Effect of the doped fibre length on soliton pulses of a bidirectional mode-locked fibre laser. Quantum Electronics, 2015, 45, 713-716.	1.0	2
749	Development of Nano-engineered Thulium-doped Fiber Laser With Low Threshold Pump Power and Tunable Operating Wavelength. IEEE Photonics Journal, 2015, , 1-1.	2.0	2
750	Passively mode-locked laser using an entirely centred erbium-doped fiber. Laser Physics, 2015, 25, 045105.	1.2	2
751	Generation of Q-Switched Mode-Locked Erbium-Doped Fiber Laser Operating in Dark Regime. Chinese Physics Letters, 2016, 33, 034201.	3.3	2
752	Dual-Wavelength Holmium-Doped Fiber Laser Pumped by Thulium–Ytterbium Co-Doped Fiber Laser. Chinese Physics Letters, 2016, 33, 054202.	3.3	2
753	Black phosphorus as a saturable absorber for generating mode-locked fiber laser in normal dispersion regime. , 2016, , .		2
754	Demonstration of passive saturable absorber by utilizing MWCNT-ABS filament as starting material. IOP Conference Series: Materials Science and Engineering, 2017, 210, 012030.	0.6	2
755	Black phosphorus saturable absorber for Q-switched technique pulse generation. , 2017, , .		2
756	Passively Q-switched of EDFL employing multi-walled carbon nanotubes with diameter less than 8 nm as saturable absorber. EPJ Web of Conferences, 2017, 162, 01014.	0.3	2

#	Article	IF	CITATIONS
757	Printed silver nanoparticles on kapton tape as passive saturable absorber. , 2017, , .		2
758	Generation of sub-nanosecond pulse in dual-wavelength praseodymium fluoride fibre laser. Laser Physics, 2019, 29, 105101.	1.2	2
759	Erbium Oxide as new Saturable Absorber for Short-Pulse Generation at 1.55-micron region. Journal of Physics: Conference Series, 2019, 1151, 012025.	0.4	2
760	NaNO3 sensing based on microfiber coated with multi-walled carbon nanotubes. Optik, 2019, 185, 936-942.	2.9	2
761	Microbottle resonator formaldehyde sensor. Journal of Physics: Conference Series, 2019, 1151, 012021.	0.4	2
762	Passively Q-switched fiber laser utilizing new hafnium–bismuth–erbium co-doped fiber as saturable absorber. Indian Journal of Physics, 2019, 93, 1489-1493.	1.8	2
763	Q-Switched Thulium-Doped Fiber Laser with Pure Titanium-Film-Based Saturable Absorber. Fiber and Integrated Optics, 2019, 38, 137-147.	2.5	2
764	Q-switched ytterbium-doped fiber laser using graphene oxide as passive saturable absorber. Journal of Physics: Conference Series, 2019, 1371, 012004.	0.4	2
765	Q-switched tunable fiber laser with aluminum oxide saturable absorber and Sagnac loop mirror. Indian Journal of Physics, 2021, 95, 1887-1893.	1.8	2
766	Rose gold nanoparticles film for generating Q-switched and mode-locked pulses. Results in Optics, 2020, 1, 100007.	2.0	2
767	PMMA microfiber and Microball Resonator for fomaldehyde liquid sensing. Sensors and Actuators A: Physical, 2020, 304, 111828.	4.1	2
768	Precursors to non-invasive clinical dengue screening: Multivariate signature analysis of in-vivo diffuse skin reflectance spectroscopy on febrile patients in Malaysia. PLoS ONE, 2020, 15, e0228923.	2.5	2
769	Passively Q-switched Ytterbium-doped fiber laser using zinc phthalocyanine thin film as saturable absorber. Optik, 2021, 228, 165736.	2.9	2
770	Effect of agarose concentration on coated microâ€bottle resonators for humidity detection. Microwave and Optical Technology Letters, 2021, 63, 1826-1831.	1.4	2
771	Gain clamping performance of Hafnia–bismuth–erbium co-doped fibre amplifier using lasing controlled structure with FBG. Journal of Modern Optics, 2021, 68, 457-462.	1.3	2
772	Applied whispering gallery modes on ZnO nanorods coated glass for humidity sensing application. Optoelectronics Letters, 2021, 17, 298-301.	0.8	2
773	Agarose coated micro-bottle sensor for relative humidity detection. Optoelectronics Letters, 2021, 17, 328-333.	0.8	2
774	Sodium Carbonate for Generating Q-Switched Pulses in 1550 nm Region. Fiber and Integrated Optics, 2021, 40, 292-303.	2.5	2

#	Article	IF	CITATIONS
775	Q-switched pulse generation in a bidirectionally pumped EDFL utilizing Lu2O3 as saturable absorber. Optoelectronics Letters, 2021, 17, 529-533.	0.8	2
776	Effect of polyvinyl alcohol coating microbottle resonator for sodium hypochlorite concentration sensing. Optik, 2021, 242, 166824.	2.9	2
777	Stretched-pulse generation in all-fiber mode-locked erbium-doped fiber laser using Lawsone dye saturable absorber. Results in Optics, 2021, 5, 100148.	2.0	2
778	Nanosecond pulse laser generation at 155 and 2  μm regions by integrating a piece of newly developed chromium-doped fiber-based saturable absorber. Applied Optics, 2019, 58, 6528.	1.8	2
779	Development of CW and Pulsed Thulium Ytterbium Co-doped Fiber Lasers Using Nano-engineered Yttria-alimina-silica Based Gain Medium in Conjunction with Cladding Pumping Technique. Current Nanoscience, 2016, 12, 299-308.	1.2	2
780	SOLITON MODE-LOCKED GENERATION BASED ON ERBIUM-DOPED FIBER LASER EMBEDDED WITH SINGLE-WALLED CARBON NANOTUBES AS SATURABLE ABSORBER. Jurnal Teknologi (Sciences and) Tj ETQq0 0 0 r	gBA /Over	læck 10 Tf 5
781	Sequential generation of self-starting diverse operations in all-fiber laser based on thulium-doped fiber saturable absorber. Chinese Physics B, 2022, 31, 064204.	1.4	2
782	Vanadium pentoxide film for microsecond pulse generation in 1.5-µm region. Optoelectronics Letters, 2022, 18, 29-34.	0.8	2
783	Broadband ASE source for S + C + L bands using hafnia-bismuth based erbium co-doped fibers. Optik, 2022, 255, 168723.	2.9	2
784	Gain flattening and clamping in L-band ring EDFA incorporating fiber Bragg grating. , 0, , .		1
785	Gain enhancement inL-band EDFA using a fiber Bragg grating. Microwave and Optical Technology Letters, 2002, 32, 388-390.	1.4	1
786	Gain and noise performances of an L-band EDFA utilizing a ring laser cavity with fiber Bragg grating. Microwave and Optical Technology Letters, 2003, 36, 1-2.	1.4	1
787	L-band gain clamped erbium-doped fiber amplifier incorporating a C/L-band WDM coupler. Microwave and Optical Technology Letters, 2004, 40, 314-316.	1.4	1
788	Gain clamped double-pass L-band EDFA with incorporation of FBG at the input end of the optical amplifier. Microwave and Optical Technology Letters, 2004, 43, 166-168.	1.4	1
789	Gain clamping in double-pass L-band EDFA using a ring resonator. Microwave and Optical Technology Letters, 2004, 43, 484-486.	1.4	1
790	Gain clamping in double-pass L-band EDFA. , 0, , .		1
791	Double-pass L-band EDFA with flat-gain and improved noise figure characteristic. , 0, , .		1
792	All-Optical Gain Clamped Double-Pass L-Band EDFA Based on Partial Reflection of ASE. IEICE Electronics Express, 2004, 1, 171-175.	0.8	1

#	Article	IF	CITATIONS
793	Gain-clamped double-pass S-band erbium-doped fiber amplifier. IEICE Electronics Express, 2005, 2, 595-599.	0.8	1
794	Dynamic dispersing technique for PR coating process in planar lightwave circuit fabrication. Microwave and Optical Technology Letters, 2007, 49, 1993-1995.	1.4	1
795	Effects of output coupler reflectivity on the performance of a linear cavity Brillouin/erbium fiber laser. Pramana - Journal of Physics, 2007, 68, 451-456.	1.8	1
796	Wide-band Bismuth based erbium doped fiber amplifier for DWDM applications. , 2009, , .		1
797	Fabrication of optical comb filter using tapered fiber based ring resonator. Proceedings of SPIE, 2010, ,	0.8	1
798	Highly efficient and high output power of erbium doped fiber laser in a linear cavity configuration. Laser Physics, 2010, 20, 1894-1898.	1.2	1
799	120nm wide band switchable fiber laser. Optics Communications, 2010, 283, 4333-4337.	2.1	1
800	Application of macro-bending for flat and broad gain EDFA. Journal of Modern Optics, 2010, 57, 1534-1541.	1.3	1
801	Filtering characteristic of the microfiber loop resonator embedded in low refractive index polymer. , 2010, , .		1
802	Quantum coherence effects in a Raman amplifier. Journal of Modern Optics, 2011, 58, 11-13.	1.3	1
803	Tunable microwave photonic frequencies generation based on stimulated Brillouin scattering operating in the Lâ€band region. Microwave and Optical Technology Letters, 2011, 53, 1710-1713.	1.4	1
804	An ultra-wideband tunable multi-wavelength Brillouin fibre laser based on a semiconductor optical amplifier and dispersion compensating fibre in a linear cavity configuration. Quantum Electronics, 2011, 41, 602-605.	1.0	1
805	Optical non-contact micrometer thickness measurement system for silica thick films. , 2012, , .		1
806	Wideband and flat-gain amplifier using high concentration Erbium doped fibers in series double-pass configuration. , 2012, , .		1
807	Microfiber structures and its sensor and laser applications. , 2012, , .		1
808	Spreading profile of evaporative liquid drops in thin porous layer. Physical Review E, 2012, 85, 016314.	2.1	1
809	Comparison of linear and ring lasers of thulium-ytterbium co-doped fiber. , 2012, , .		1
810	Flat-Gain Single-Stage Amplifier Using High Concentration Erbium Doped Fibers in Single-Pass and		1

Double-Pass Configurations. , 2012, , .

#	Article	IF	CITATIONS
811	Demonstration of DC current sensing through Microfiber Knot Resonator. , 2012, , .		1
812	Dual-cavity dual-output multi-wavelength fiber laser based on nonlinear polarization rotation effect. Laser Physics, 2012, 22, 1601-1605.	1.2	1
813	Modeling and experimental analysis of wide-band flat-gain amplifier utilizing high concentration of EDFA. , 2012, , .		1
814	Investigation on threshold power of stimulated Brillouin scattering in photonic crystal fiber. Optik, 2012, 123, 1149-1152.	2.9	1
815	Enhancement of Brillouin Stokes generation in the S-band region using a combination S-band Depressed Cladding Erbium Doped Fiber and Semiconductor Optical Amplifier. Laser Physics, 2012, 22, 598-604.	1.2	1
816	S + C + L Band tunable wavelength conversion using FWM dualâ€wavelength fiber laser in a highly nonlinear fiber. Microwave and Optical Technology Letters, 2013, 55, 379-382.	1.4	1
817	High resolution interrogation system for fiber Bragg grating (FBG) sensor application using radio frequency spectrum analyser. , 2013, , .		1
818	Brillouin erbium fiber laser generation in a figure-of-eight configuration with double brillouin frequency spacing. , 2013, , .		1
819	S – C – L triple wavelength superluminescent source based on an ultra-wideband SOA and FBGs. Quantum Electronics, 2013, 43, 923-926.	1.0	1
820	Nonadiabatic microfiber based mode″ocked erbiumâ€doped fiber laser using graphene. Microwave and Optical Technology Letters, 2014, 56, 1670-1673.	1.4	1
821	Mode-locked thulium bismuth codoped fiber laser using graphene saturable absorber in ring cavity: reply. Applied Optics, 2014, 53, 555.	1.8	1
822	Square pulse emission with ultraâ€low repetition rate utilising nonâ€linear polarisation rotation technique. Journal of Engineering, 2014, 2014, 517-521.	1.1	1
823	Enhanced performance of an S-band fiber laser using a thulium-doped photonic crystal fiber. Laser Physics, 2014, 24, 115201.	1.2	1
824	Thulium Bismuth Co-Doped Fiber Lasers at 1901 nm by 802 nm Pumping. IEEE Journal of Selected Topics in Quantum Electronics, 2014, 20, 132-137.	2.9	1
825	Supercontinuum generation from a sub-megahertz repetition rate femtosecond pulses based on nonlinear polarization rotation technique. Journal of Modern Optics, 2014, 61, 1333-1338.	1.3	1
826	Electrostatic charge interaction: a case study on tapered PMMA fiber for calcium nitrate detection. Sensor Review, 2014, 34, 424-427.	1.8	1
827	Investigation of thermal effects in a resonance condition of microfibre doubleâ€knot resonators as highâ€order filter. Micro and Nano Letters, 2015, 10, 580-582.	1.3	1
828	Four wave mixing techniques in measuring HNLF. AIP Conference Proceedings, 2015, , .	0.4	1

#	Article	IF	CITATIONS
829	Observation violet emission of microfiber knot resonator. Microwave and Optical Technology Letters, 2015, 57, 2929-2931.	1.4	1
830	Fiber Bragg grating sensor for humidity measurement. , 2015, , .		1
831	Investigation of nitrogen doped graphene as saturable absorber in Thulium-Doped Fiber Laser. , 2015, , .		1
832	Influence of design parameters on the performance of a refractive index sensor based on SPR in plastic optical fibers. , 2015, , .		1
833	Enhancement of Thulium–Ytterbium doped fiber laser efficiency using dualâ€pumping method. Microwave and Optical Technology Letters, 2015, 57, 285-287.	1.4	1
834	Comparison of cladding shaped of Tm/Yb doped fiber laser for optimum lasing efficiency. , 2016, , .		1
835	Realization of spectral tunable filter based on thermal effect in microfiber structure. Optical Fiber Technology, 2016, 28, 38-41.	2.7	1
836	Mode-locking pulse generation in cladding pumped Erbium-Ytterbium co-doped fiber laser with graphene PVA film. Optik, 2017, 136, 531-535.	2.9	1
837	Relative humidity sensor based on MWCNTs-doped polymer microfiber. , 2017, , .		1
838	Erbium-Doped Zirconia-Alumina Silica Glass-Based Fiber as a Saturable Absorber for High Repetition Rate Q-Switched All-Fiber Laser Generation. Chinese Physics Letters, 2017, 34, 084203.	3.3	1
839	All-fibre Q-switching YDFL operation with bismuth-doped fibre as saturable absorber. Journal of Modern Optics, 2018, 65, 946-950.	1.3	1
840	Nickel Oxide as a Q-switcher for Short Pulsed Thulium Doped Fiber Laser Generation. Journal of Physics: Conference Series, 2019, 1151, 012029.	0.4	1
841	Bismuth (III) Telluride-Polyethylene Oxide as passive saturable absorber. Journal of Physics: Conference Series, 2019, 1151, 012002.	0.4	1
842	Passively Q-switched Erbium doped fiber laser by incorporating a segment of Thulium doped fiber saturable absorber. Journal of Physics: Conference Series, 2019, 1151, 012010.	0.4	1
843	Polymer microfiber coated with ZnO for humidity sensing. Journal of Physics: Conference Series, 2019, 1151, 012019.	0.4	1
844	Microsecond pulse erbium-doped fiber laser using WS2 deposited on D-shaped fiber fabricated by polishing wheel technique. Journal of Physics: Conference Series, 2019, 1371, 012001.	0.4	1
845	Optimization of ZnO nanorods growth duration for humidity sensing application. Journal of Physics: Conference Series, 2019, 1371, 012005.	0.4	1
846	A study of relative humidity sensor on micro-ball resonator. Journal of Physics: Conference Series, 2019, 1371, 012009.	0.4	1

#	Article	IF	CITATIONS
847	Passively Femtosecond Mode-Locked Erbium-Doped Fiber Oscillator with External Pulse Compressor for Frequency Comb Generation. Journal of Optical Communications, 2024, 44, s683-s690.	4.7	1
848	Samarium (III) oxide thin film as a saturable absorber for the passively Q-switched Tm-doped fiber laser. Journal of Physics: Conference Series, 2019, 1371, 012026.	0.4	1
849	Alq 3 saturable absorber for generating Qâ€switched pulses in erbiumâ€doped fiber laser. Microwave and Optical Technology Letters, 2020, 62, 1028-1032.	1.4	1
850	Non-contact Fiber Optic Displacement Sensor for Sugar Concentration Detection. Journal of Physics: Conference Series, 2020, 1484, 012006.	0.4	1
851	D-shape Fiber Coated with Indium Tin Oxide for Temperature Sensor Application. IOP Conference Series: Materials Science and Engineering, 2020, 854, 012016.	0.6	1
852	Humidity Effects on the Growth of ZnO Nanorods using Hydrothermal Method. Journal of Physics: Conference Series, 2020, 1552, 012004.	0.4	1
853	Optimizing waist diameter of microfiber-ZnO nanorods structure for humidity sensing application. AlP Conference Proceedings, 2020, , .	0.4	1
854	Efficiency enhancement of phase-conjugated twin waves technique by shaping envelopes of subcarriers in all-optical OFDM systems. Optics Communications, 2020, 472, 125864.	2.1	1
855	Q-switched tunable fiber laser utilizing silver nanoparticles deposited onto PVA film as saturable absorber. Indian Journal of Physics, 2021, 95, 141-145.	1.8	1
856	Passively Q-Switched Pulses Generation from Erbium-Doped Fiber Laser Using Lutetium Oxide as Saturable Absorber. Journal of Microwaves, Optoelectronics and Electromagnetic Applications, 2021, 20, 118-125.	0.7	1
857	HEC/PVDF coated microbottle resonators for relative humidity detection. Optik, 2021, 232, 166534.	2.9	1
858	Acetone Liquid Sensing Based on Fiber Optic Mach-Zehnder Interferometer. , 2021, , .		1
859	Micro-bottle resonator for sodium hypochlorite sensor. Optik, 2021, 242, 167328.	2.9	1
860	Concentration measurement of opaque dye solution using a non-contact fiber displacement sensor. Optical Fiber Technology, 2021, 65, 102624.	2.7	1
861	Highly Efficient Cladding Pumped Dual-Wavelength Thulium Ytterbium Co-Doped Fiber Laser. Acta Physica Polonica A, 2016, 130, 1332-1335.	0.5	1
862	Q-switched fiber laser with tungsten disulfide saturable absorber prepared by drop casting method. Photonics Letters of Poland, 2017, 9, 103.	0.4	1
863	Optical properties enhancement with multilayer coating technique of additiveâ€enhanced zinc oxide nanostructure for fiber <scp>Bragg</scp> grating humidity sensor. Microwave and Optical Technology Letters, 2022, 64, 184-189.	1.4	1
864	Double Pass L-Band EDFA with Unpumped EDF. , 2002, , .		1

864 Double Pass L-Band EDFA with Unpumped EDF. , 2002, , .

#	Article	IF	CITATIONS
865	Dark Pulse Mode-locked Laser based on Aluminum Zinc Oxide coated D-shape fiber as Saturable Absorber. Fiber and Integrated Optics, 2021, 40, 322-334.	2.5	1
866	Surface plasmon resonance optical sensor for COVID-19 detection. Nanosystems: Physics, Chemistry, Mathematics, 2021, 12, 575-582.	0.4	1
867	The generation of nanosecond pulses at C-band region with titanium dioxide as a saturable absorber. Journal of Physics: Conference Series, 2021, 2075, 012013.	0.4	1
868	Iron pyrite absorber for ultrashort pulse generation. Infrared Physics and Technology, 2022, 120, 103999.	2.9	1
869	Photonâ \in toâ \in photon polarization modulation using Mxene thin film as modulator. Electronics Letters, 0, , .	1.0	1
870	Graphene Oxide/Gold Coated Kretschmann Surface Plasmon Resonance Setup for Relative Humidity Detection. , 2022, 6, 1-4.		1
871	Picosecond Soliton Pulse Generation with a Zinc Phthalocyanine Thin-Film Saturable Absorber Via Mode Locking in an Erbium-Doped Fiber Laser Cavity. Journal of Russian Laser Research, 2022, 43, 193.	0.6	1
872	Tungsten disulfide coated sideâ€polished fibre as polarisation state modulator in allâ€optical system. IET Optoelectronics, 0, , .	3.3	1
873	Titanium Carbide MXene as a Mode Locker in Erbium-Doped Fiber Laser Cavity. Journal of Russian Laser Research, 0, , .	0.6	1
874	Q-Switched Fiber Laser with a Hafnium-Bismuth-Erbium Codoped Fiber as Gain Medium and Sb2Te3 as Saturable Absorber. Journal of Russian Laser Research, 0, , .	0.6	1
875	Rare-earth Yttrium oxide as Q-switcher in fiber laser system. Results in Optics, 2022, 8, 100252.	2.0	1
876	Gain-clamped erbium-doped fiber amplifier using a single fiber Bragg grating. Microwave and Optical Technology Letters, 2001, 29, 290-293.	1.4	0
877	Highly Efficient L-Band Erbium-Doped Fiber Amplifier with Unpumped Erbium-Doped Fiber in Double Pass Configuration. Japanese Journal of Applied Physics, 2002, 41, L833-L835.	1.5	0
878	Gain Control in L-Band Erbium-Doped Fiber Amplifier Incorporating Broadband Fiber Bragg Grating. Japanese Journal of Applied Physics, 2002, 41, L1459-L1460.	1.5	0
879	Hybrid Brillouin/Erbium fibre laser operating at long wavelength band. Microwave and Optical Technology Letters, 2002, 33, 383-385.	1.4	0
880	10-GHz Optical Comb in L-Band Region With Brillouin/Erbium-Doped Fibre Laser. Optical Review, 2003, 10, 133-135.	2.0	0
881	Double pass L-band EDFA with an improved gain coefficient. , 0, , .		0

6882 Gain clamping in dual-stage L-band EDFA by recycling a backward ASE. , 0, , .

0

#	Article	IF	CITATIONS
883	Two-stage L-band erbium doped fiber amplifier. , 0, , .		Ο
884	Enhancement of Gain in L-Band Bismuth-Based Erbium-Doped Fibre Amplifier Using an Un-pumped EDF and Midway Isolator. Chinese Physics Letters, 2004, 21, 2452-2453.	3.3	0
885	Effect of Recycling a Backward Ase on Performance of Double Pass L-Band Edfa. Journal of Optics (India), 2004, 33, 181-186.	1.7	Ο
886	L-BAND EDFA WITH INJECTION OF C-BAND ASE. Journal of Nonlinear Optical Physics and Materials, 2004, 13, 315-319.	1.8	0
887	Gain clamping in double-pass L-band EDFA using a broadband FBG. Pramana - Journal of Physics, 2004, 62, 893-897.	1.8	0
888	Effect of coupling ratio on performance of self-excited Brillouin/erbium fiber laser. IEICE Electronics Express, 2004, 1, 460-464.	0.8	0
889	DOUBLE PASS S-BAND EDFA. Journal of Nonlinear Optical Physics and Materials, 2006, 15, 303-307.	1.8	0
890	Inductively coupled plasma of fluorocarbon plasma glass etching process on planar lightwave circuit device fabrication. , 2007, , .		0
891	An efficient EYDFA with a 54 dB small signal gain. Microwave and Optical Technology Letters, 2007, 49, 2337-2339.	1.4	0
892	All-optical Gain-clamped Erbium-doped Fiber Amplifier with Narrowband Amplified Spontaneous Emission Feedback Technique. Journal of Optical Communications, 2008, 29, .	4.7	0
893	Enhancement of four wave mixing characteristic in Semiconductor Optical Amplifier using Fiber loop mirror. , 2009, , .		0
894	An efficient double-pass Bismuth-based erbium-doped fiber amplifier. , 2009, , .		0
895	An Erbium -Ytterbium DFB laser with a simple and compact structure. Journal of Physics: Conference Series, 2009, 187, 012003.	0.4	Ο
896	SINGLE MODE ERBIUM YTTERBIUM-DOPED FIBER LASER WITH MULTIMODE PUMPING. Journal of Nonlinear Optical Physics and Materials, 2010, 19, 203-208.	1.8	0
897	Numerical study of macro bending effect on high concentration EDFA. , 2010, , .		0
898	Investigation on the nonlinear parameters of a photonic crystal fiber by four-wave mixing. , 2010, , .		0
899	Microfiber-based devices: Current sensor and tunable laser. , 2011, , .		0
900	Numerical Modelling of C-Band Bismuth-Based Erbium Doped Amplifier. , 2011, , .		0

Numerical Modelling of C-Band Bismuth-Based Erbium Doped Amplifier. , 2011, , . 900

#	Article	IF	CITATIONS
901	Dual-wavelength tunable fibre laser with a 15-dBm peak power. Quantum Electronics, 2011, 41, 709-714.	1.0	Ο
902	DUAL WAVELENGTH HIGH POWER DOUBLE-CLAD ERBIUM/YTTERBIUM-DOPED FIBER LASER. Journal of Nonlinear Optical Physics and Materials, 2011, 20, 443-451.	1.8	0
903	20 GHz Optical Combs Generation in Brillouin Fiber Laser with a Compact Ring Cavity. , 2011, , .		0
904	Publisher's Note: Spreading profile of evaporative liquid drops in thin porous layer [Phys. Rev. E85, 016314 (2012)]. Physical Review E, 2012, 85, .	2.1	0
905	Microfiber coupler devices. , 2012, , .		0
906	Wideband spectrum-sliced ASE source operating at 2 micron region based on double clad ytterbium-sensitized thulium-doped fiber. , 2012, , .		0
907	System tolerance of NRZ-DQPSK all-optical OFDM in long-haul transmission system using DCF. , 2012, , .		0
908	A new fiber optic salinity sensing device based on beam-through technique. , 2012, , .		0
909	The effects of placement and geometry on thermo-pneumatic pumping on centrifugal microfluidic compact disc (CD) platforms. , 2012, , .		Ο
910	All-fiber graphene passively Q-switched nanosecond Thulium doped fiber laser at 1900 nm. , 2013, , .		0
911	Closely Spaced, Dualâ€SIm Fiber Laser for Microwave Generation With A Single Fbg. Microwave and Optical Technology Letters, 2013, 55, 2011-2015.	1.4	Ο
912	Comparison between the single and dual-pumping method of large mode area Yb ³⁺ /Tm ³⁺ co-doped air-clad fiber laser. , 2013, , .		0
913	Stability analysis in a soliton fiber ring laser with a hybrid saturable absorber. Microwave and Optical Technology Letters, 2013, 55, 164-170.	1.4	Ο
914	Fiber optic displacement sensor for scanning and reconstructing occlusal surface of human tooth. , 2013, , .		0
915	1.9 μm lasing with Tm ³⁺ /Yb ³⁺ coâ€doped airâ€clad fiber and 931 nm pumping. Microwave and Optical Technology Letters, 2013, 55, 1124-1126.	1.4	Ο
916	Controllable stretched pulse and dissipative soliton emission using nonâ€linear polarisation rotation and cavity loss tuning mechanism. IET Optoelectronics, 2013, 7, 38-41.	3.3	0
917	Switchable pulse and multi-wavelength laser based on non-linear polarization rotation. , 2013, , .		0
918	1.9~2 μm gain shifted TBDFA employing different Tm-Bi concentration ratio. , 2014, , .		0

#	Article	IF	CITATIONS
919	Brillouin Lasing with a Reduced Self-Pulsing Characteristic Using a Short-Length Erbium-Doped Fiber as the Nonlinear Gain Medium. Chinese Physics Letters, 2014, 31, 054202.	3.3	0
920	Closely spaced dual-wavelength fiber laser using an ultranarrow bandwidth optical filter for low radio frequency generation. Applied Optics, 2014, 53, 4123.	1.8	0
921	Q-SWITCHED THULIUM-DOPED FIBER LASER AT 2 MICRON REGION BY 802 NM PUMPING. Jurnal Teknologi (Sciences and Engineering), 2015, 74, .	0.4	0
922	Generation of Cubic-Quintic nonlinear schrödinger equation dark pulse. , 2015, , .		0
923	Fundamental and harmonic soliton mode-locked erbium-doped fiber laser using a single-walled carbon nanotubes embedded in poly (ethylene oxide) film saturable absorber. Proceedings of SPIE, 2015, , .	0.8	0
924	A WIDEBAND AND FLAT-GAIN OF AN AMPLIFIER BY USING ZIRCONIA-BASED ERBIUM-DOPED FIBER (ZR-EDF) FOR SINGLE PASS PPERATION. Jurnal Teknologi (Sciences and Engineering), 2016, 78, .	0.4	0
925	GRAPHENE OXIDE-POLYETHYLENE OXIDE (PEO) FILM AS SATURABLE ABSORBER ON MODE-LOCKED ERBIUM DOPED FIBER LASER GENERATION. Jurnal Teknologi (Sciences and Engineering), 2016, 78, .	0.4	0
926	Multi-wavelength Brillouin Erbium Fiber laser with Pulsing characteristics. , 2016, , .		0
927	Generating 2 micron continuous-wave ytterbium-doped fiber laser-based optical parametric effect. Laser Physics Letters, 2016, 13, 105109.	1.4	0
928	Graphene Oxide saturable absorber for generating eye-safe Q-switched fiber laser. IOP Conference Series: Materials Science and Engineering, 2017, 210, 012042.	0.6	0
929	Ultrafast soliton mode-locked Zirconia-based Erbium-doped fiber laser with carbon nanotubes saturable absorber. IOP Conference Series: Materials Science and Engineering, 2017, 210, 012051.	0.6	0
930	Continues-wave Brillouin-Raman fiber ring laser using 7.7 km long dispersion compensating fiber at 1563 nm wavelength. IOP Conference Series: Materials Science and Engineering, 2017, 210, 012047.	0.6	0
931	Investigation of Brillouin Raman fiber laser operating at 1558 nm using THDF saturable absorber. IOP Conference Series: Materials Science and Engineering, 2017, 210, 012048.	0.6	0
932	Q-switched erbium doped fiber laser using antimony telluride-polyvinyl alcohol (Sb2Te3-PVA) as saturable absorber. EPJ Web of Conferences, 2017, 162, 01011.	0.3	0
933	1563 nm Q-Switched Brillouin-Raman fiber laser using Graphene as a saturable absorber. IOP Conference Series: Materials Science and Engineering, 2017, 210, 012055.	0.6	0
934	Q-switched double-clad Ytterbium-doped fiber laser using MoS2flakes saturable absorber. IOP Conference Series: Materials Science and Engineering, 2017, 210, 012054.	0.6	0
935	Generation of an ultrafast femtosecond soliton fiber laser by carbon nanotube as saturable absorber. Journal of Physics: Conference Series, 2018, 1027, 012011.	0.4	0
936	Nickel oxide nanoparticles for Q-switching pulses generation. Journal of Physics: Conference Series, 2019, 1151, 012027.	0.4	0

#	Article	IF	CITATIONS
937	Mode-locked Pulsed Fiber Laser with Graphene Solution as Saturable Absorber Deposited in Photonic Crystal Fiber. , 2019, , .		0
938	Q-Switched dual-wavelength erbium-doped fiber laser using graphene as a saturable absorber. Journal of Physics: Conference Series, 2019, 1371, 012007.	0.4	0
939	PMMA microball resonator for formaldehyde liquid sensing. Journal of Physics: Conference Series, 2019, 1371, 012012.	0.4	Ο
940	Q-switched Thulium-doped fiber laser with Bismuth-doped fiber saturable absorber. Journal of Physics: Conference Series, 2019, 1371, 012024.	0.4	0
941	Q-switching Zirconia-Erbium-doped Pulsed Fiber Laser with MWCNTs-PEO as Saturable Absorber. Journal of Physics: Conference Series, 2019, 1372, 012003.	0.4	0
942	Q-switched Thulium-doped fibre laser using Bismuth (III) Telluride-based saturable absorber. Journal of Physics: Conference Series, 2019, 1371, 012008.	0.4	0
943	Microsecond Pulse Generation using Bismuth Salenide as Saturable Absorber in 1.5 μm Region. IOP Conference Series: Materials Science and Engineering, 2020, 854, 012037.	0.6	0
944	Q-switched Erbium-Doped Fiber Laser Incorporating Multi-Walled Carbon Nanotubes as a Saturable Absorber. IOP Conference Series: Materials Science and Engineering, 2020, 854, 012059.	0.6	0
945	Fibre-based Saturable Absorbers for Pulsed Generations in the 1-micron Region. IOP Conference Series: Materials Science and Engineering, 2020, 854, 012071.	0.6	0
946	Passively Q-switched Erbium-doped Fiber Laser using Tungsten Disulfide deposited D-shaped Fiber as Saturable Absorber. IOP Conference Series: Materials Science and Engineering, 2020, 854, 012021.	0.6	0
947	Reductionâ€controlled graphene oxide saturable absorbers and its effect on ultrashort Erâ€doped fibre laser. IET Optoelectronics, 2021, 15, 61-68.	3.3	0
948	Simple Fabrication of Bismuth Telluride Used as Saturable Absorber for Generating Microsecond Pulse Fiber Laser. , 2021, , .		0
949	Titanium carbide MXene for generating Qâ€switched pulses in erbiumâ€doped fiber laser cavity. Microwave and Optical Technology Letters, 2021, 63, 2893-2897.	1.4	0
950	Gainâ€clamping in Lâ€band zirconium–erbium coâ€doped fiber amplifier with FBG based lasing control. Microwave and Optical Technology Letters, 2022, 64, 389.	1.4	0
951	Efficient and Compact Optical Amplifier Using EYDF. IIUM Engineering Journal, 2010, 8, 17-23.	0.8	0
952	Q-Switched Erbium-Doped Fiber Laser Based on Nonlinear Polarisation Rotation Technique. Journal of Nanoelectronics and Optoelectronics, 2014, 9, 525-528.	0.5	0
953	AMPLIFICATION AND LASING CHARACTERISTICS OF THULIUM YTTERBIUM CO-DOPED FIBER. Jurnal Teknologi (Sciences and Engineering), 2015, 74, .	0.4	0
954	GENERATION OF Q-SWITCHED THULIUM-DOPED FIBER LASER (TDFL) USING DIFFERENTSATURABLE ABSORBERS. Jurnal Teknologi (Sciences and Engineering), 2016, 78, .	0.4	0

#	Article	IF	CITATIONS
955	Switchable Brillouin frequency multiwavelength and pulsed fiber laser. Chinese Optics Letters, 2017, 15, 101401.	2.9	0
956	Enhanced Relative Humidity Sensing Based on a Tapered Fiber Bragg Grating with Zinc Oxide Nanostructure-Embedded Coatings. Advanced Science Letters, 2017, 23, 5452-5456.	0.2	0
957	Detection of Honey Adulteration by Addition of Glucose via a Microfiber Coupler. Advanced Science Letters, 2017, 23, 5561-5564.	0.2	0
958	Formaldehyde sensing using micro-loop resonator. AIP Conference Proceedings, 2020, , .	0.4	0
959	Relative Humidity Sensor based on Tapered Plastic Optical Fibre with Full-and Spiral-Patterned Agarose Gel Coating. , 2020, , .		0
960	Hafnium Bismuth Erbium Co-Doped Fiber Based Dark Pulses Generation With Black Phosphorus As Saturable Absorber. Journal of Physics: Conference Series, 2021, 2075, 012018.	0.4	0
961	Q-switched Ytterbium-doped fibre laser using an 8 cm long Hafnium bismuth erbium co-doped fibre saturable absorber. Journal of Physics: Conference Series, 2021, 2075, 012020.	0.4	0
962	Generation of Passive Q-switched by using Graphene Oxide in Erbium Doped Fiber Laser. , 2021, , .		0
963	The Design of Optical Waveguide Sensor Based on Surface Plasmon Resonance. , 2021, , .		0
964	Characteristics of the 11-Mercaptoundecanoic Acid (11-MUA) Binding to Gold Surface as Self-Assembled Monolayer (SAM) for SPR based Biosensor. , 2022, , .		0